Iranian Journal of Numerical Analysis and Optimization

Volume 3 , Number 2

Summer 2013

Ferdowsi University of Mashhad, Iran

In the Name of God

Iranian Journal of Numerical Analysis and Optimization (IJNAO)

This journal is authorized under the registration No. 174/853 dated 1386/2/26, by the Ministry of Culture and Islamic Guidence.

Volume 3, Number 2, Summer 2013

ISSN: 1735-7144

Publisher: Faculty of Mathematical Sciences, Ferdowsi University of Mashhad

Published by: Ferdowsi University of Mashhad Press

Circulation: 250

Address: Iranian Journal of Numerical Analysis and Optimization

Faculty of Mathematical Sciences

Ferdowsi University of Mashhad

P.O. Box 1159, Mashhad 91775, Iran.

Tel-Fax: +98-511-8828606

E-mail: mjms@um.ac.ir

Website: http://jm.um.ac.ir/index.php/math

This journal is indexed by:

• Mathematical Review

• Zenteralblatt

In the Name of God

Iranian Journal of Numerical Analysis and Optimization

Volume 3, Number 2, Summer 2013

Ferdowsi University of Mashhad - Iran

Iranian Journal of Numerical Analysis and Optimization

University of Technology, Tehran.
e-mail: nezamm@sina.sharif.edu
Salehi Fathabadi, H.*
(Operations Research)
School of Mathematics, Statistics and
Computer Sciences,
University of Tehran, Tehran.
e-mail: hsalehi@ut.ac.ir
Soheili, A.*
(Numerical Analysis)
Department of Applied Mathematics,
Ferdowsi University of Mashhad, Mashhad.
e-mail: soheili@um.ac.ir
Taghizadeh Kakhki, H.**
(Operations Research)
Department of Applied Mathematics,
Ferdowsi University of Mashhad, Mashhad.
e-mail: taghizad@math.um.ac.ir
Toutounian, F.*
(Numerical Analysis)
Department of Applied Mathematics,
Ferdowsi University of Mashhad, Mashhad.
e-mail: toutouni@math.um.ac.ir

This journal is published under the auspices of Ferdowsi University of Mashhad

---

* Full Professor

** Associate Professor

Letter from the Editor in Chief

I would like to welcome you to the Iranian Journal of Numerical Analysis and Optimization (IJNAO). This journal is published biannually and supported by the Faculty of Mathematical Sciences at the Ferdowsi University of Mashhad. Faculty of Mathematical Sciences with three centers of excellence and three research centers is well-known in mathematical communities in Iran.
The main aim of the journal is to facilitate discussions and collaborations between specialists in applied mathematics, especially in the fields of numerical analysis and optimization, in the region and worldwide.
Our vision is that scholars from different applied mathematical research disciplines, pool their insight, knowledge and efforts by communicating via this international journal.
In order to assure high quality of the journal, each article will be reviewed by subject-qualified referees.
Our expectations for IJNAO are as high as any well-known applied mathematical journal in the world. We trust that by publishing quality research and creative work, the possibility of more collaborations between researchers would be provided. We invite all applied mathematicians especially in the fields of numerical analysis and optimization to join us by submitting their original work to the Iranian Journal of Numerical Analysis and Optimization.

Mohammad Hadi Farahi

Contents

Iranian J. of Numerical Anal sis and Optimization
Vol 3, No. 2, 2013 , pp 1-12

Hopf bifurcation analysis of a delayed five-neuron BAM neural network with two neurons in the X-layer

. Javidmanesh and Z. Afsharnezhad

Abstract

In this paper, a bidirectional associative memor BAM neural net ork, hich consists of t o neurons in the X-la er and three neurons in the Y-la er, ith t o time dela s ill be studied. We conclude that under some assumptions, Hopf bifurcation occurs hen the sum of t o dela s passes through a critical value. A numerical example is presented to support our theoretical results.

ey ords: Neural network; Hopf bifurcation; Characteristic equation; Time delay.

1 Introduction

The attention of many scientists (eg., mathematicians, physicists, computer scientists, engineers and so on) have been attracted toward the dynamical characteristics of artificial neural networks since Hopfield constructed a simplified neural network (NN) model [1]. As time delays always occur in the signal transmission, Marcus and Westervelt proposed an NN model with delay [2]. Many dynamical behaviours such as periodic phenomenon, bifurcation and chaos have been discussed on these systems (e.g. [3, 4, 5, 6, 7, 8, 9, 2, 10]).

The bidirectional associative memory (BAM) networks were first introduced by asko (e.g. [11, 12]). The properties of periodic solutions are significant in many applications. It is well known that BAM NNs are able to store multiple patterns, but most of NNs have only one storage pattern or memory pattern. BAM NNs have practical applications in storing paired patterns or memories and have the ability of searching the desired patterns through both forward and backward directions.

Recieved 20 Februar 2013; accepted 11 June 2013
E. Javidmanesh
Department of Applied Mathematics, Ferdo si niversit of Mashhad, Mashhad, Iran.
e-mail e_ avidmanesh ahoo.com

Z. Afsharnezhad
Department of Applied Mathematics, Ferdo si niversit of Mashhad, Mashhad, Iran.
e-mail afsharnezhad um.ac.ir

The delayed BAM neural network is described by the following system:

$$\begin{cases} \dot{x_i}(t) = -\mu_i x_i(t) + \sum_{j=1}^{m} c_{ji} f_i(y_j(t-\tau_{ji})) + I_i \quad (i = 1, 2, \ldots, n) \\ \dot{y_j}(t) = -\upsilon_j y_j(t) + \sum_{i=1}^{n} d_{ij} g_j(x_i(t-\sigma_{ij})) + J_j \ (j = 1, 2, \ldots, m) \end{cases} \tag{1}$$

where c_{ji} and d_{ij} are the connection weights through the neurons in two layers: the X-layer and the Y-layer. The stability of internal neuron processes on the X-layer and Y-layer are described by μ_i and υ_j, respectively. On the X-layer, the neurons whose states are denoted by $x_i(t)$ receive the input I_i and the inputs outputted by those neurons in the Y-layer via activation function f_i, while the similar process happens on the Y-layer. Also, τ_{ji} and σ_{ij} correspond to the finite time delays of neural processing and delivery of signals. For further details, we refer to [12, 11].

Since a great number of periodic solutions indicate multiple memory patterns, the study of Hopf bifurcation is very important for the design and application of BAM NNs. In fact, various local periodic solutions can arise from the different equilibrium points of BAM NNs by applying Hopf bifurcation technique. But the exhaustive analysis of the dynamics of such a large system is complicated, so some authors have studied the dynamical behaviours of simplified systems. For example, the simplified three-neuron, four-neuron, five-neuron and six-neuron BAM NNs with multiple delays have been studied in [13, 14, 6, 15, 8, 9, 16, 17, 10, 18, 19, 20]. It should be noted that in the above papers, the systems which have been considered, just consist of one neuron in the X-layer and other neurons in the Y-layer. This way of choosing the systems simplifies the analysis. Also, [20] studied the stability and local Hopf bifurcation of a five-neuron ring neural network with delays and self connection. However, there are many other forms of BAM NNs that have not been studied.

Motivated by the above, in this paper, we consider the following five-neuron BAM neural network. We should point out that in [21], the following system has been studied through center manifold theory, but here, we study this system according to the distribution of roots. In [14], a more simplified form of (2) with some assumptions has been considered, but they have stated some results of synchronization.

$$\begin{cases} \dot{x_1}(t) = -\mu_1 x_1(t) + c_{11} f_1(y_1(t-\tau_2)) + c_{21} f_1(y_2(t-\tau_2)) \\ \qquad\quad +c_{31} f_1(y_3(t-\tau_2)) \\ \dot{x_2}(t) = -\mu_2 x_2(t) + c_{12} f_2(y_1(t-\tau_2)) + c_{22} f_2(y_2(t-\tau_2)) \\ \qquad\quad +c_{32} f_2(y_3(t-\tau_2)) \\ \dot{y_1}(t) = -\upsilon_1 y_1(t) + d_{11} g_1(x_1(t-\tau_1)) + d_{21} g_1(x_2(t-\tau_1)) \\ \dot{y_2}(t) = -\upsilon_2 y_2(t) + d_{12} g_2(x_1(t-\tau_1)) + d_{22} g_2(x_2(t-\tau_1)) \\ \dot{y_3}(t) = -\upsilon_3 y_3(t) + d_{13} g_3(x_1(t-\tau_1)) + d_{23} g_3(x_2(t-\tau_1)) \end{cases} \tag{2}$$

where $\mu_i > 0 (i = 1, 2)$, $\upsilon_j > 0 (j = 1, 2, 3)$, $c_{j1}, c_{j2} (j = 1, 2, 3)$ and $d_{i1}, d_{i2}, d_{i3} (i = 1, 2)$ are real constants. The time delay from the X-layer

to another Y-layer is τ_1, while the time delay from the Y-layer back to the X-layer is τ_2, and there are two neurons in the X-layer and three neurons in the Y-layer. First, we take the sum of the delays $\tau = \tau_1 + \tau_2$ as parameter and we will show that the zero solution loses its stability and Hopf bifurcation occurs when τ passes through a critical value.

This paper is organized in four sections. In section 2, we will analyze the stability and Hopf bifurcation. To illustrate the results, numerical simulation is presented in section 3. Finally, in section 4, some main conclusions are stated.

2 Stability analysis and Hopf bifurcation

First, we need to explain some transformations stated in [21]. Letting $u_1(t) = x_1(t-\tau_1)$, $u_2(t) = x_2(t-\tau_1)$, $u_3(t) = y_1(t)$, $u_4(t) = y_2(t)$, $u_5(t) = y_3(t)$ and $\tau = \tau_1 + \tau_2$, system (2) can be rewritten as the following equivalent system:

$$\begin{cases} \dot{u_1}(t) = -\mu_1 u_1(t) + c_{11} f_1(u_3(t-\tau)) + c_{21} f_1(u_4(t-\tau)) \\ \qquad\quad +c_{31} f_1(u_5(t-\tau)) \\ \dot{u_2}(t) = -\mu_2 u_2(t) + c_{12} f_2(u_3(t-\tau)) + c_{22} f_2(u_4(t-\tau)) \\ \qquad\quad +c_{32} f_2(u_5(t-\tau)) \\ \dot{u_3}(t) = -\upsilon_1 u_3(t) + d_{11} g_1(u_1(t)) + d_{21} g_1(u_2(t)) \\ \dot{u_4}(t) = -\upsilon_2 u_4(t) + d_{12} g_2(u_1(t)) + d_{22} g_2(u_2(t)) \\ \dot{u_5}(t) = -\upsilon_3 u_5(t) + d_{13} g_3(u_1(t)) + d_{23} g_3(u_2(t)) \end{cases} \tag{3}$$

To establish the main results for system (3), it is necessary to make the following assumption:

$$\text{(H1) } f_i, g_j \in C^1,\ f_i(0) = g_j(0) = 0,\ (i = 1, 2;\ j = 1, 2, 3).$$

Note that the above assumption is necessary for linearization. It is easily seen that the origin $(0, 0, 0, 0, 0)$ is an equilibrium point of (3). Under the hypothesis (H1), the linearization of (3) at $(0, 0, 0, 0, 0)$ is

$$\begin{cases} \dot{u_1}(t) = -\mu_1 u_1(t) + \alpha_{31} u_3(t-\tau) + \alpha_{41} u_4(t-\tau) + \alpha_{51} u_5(t-\tau) \\ \dot{u_2}(t) = -\mu_2 u_2(t) + \alpha_{32} u_3(t-\tau) + \alpha_{42} u_4(t-\tau) + \alpha_{52} u_5(t-\tau) \\ \dot{u_3}(t) = -\upsilon_1 u_3(t) + \alpha_{13} u_1(t) + \alpha_{23} u_2(t) \\ \dot{u_4}(t) = -\upsilon_2 u_4(t) + \alpha_{14} u_1(t) + \alpha_{24} u_2(t) \\ \dot{u_5}(t) = -\upsilon_3 u_5(t) + \alpha_{15} u_1(t) + \alpha_{25} u_2(t) \end{cases} \tag{4}$$

where $\alpha_{mi} = c_{ki} f_i'(0)$, $\alpha_{im} = d_{ik} g_k'(0)$ for $m = 3, 4, 5$, $k = m - 2$, $i = 1, 2$. Then the associated characteristic equation of (4) is

$$det\begin{pmatrix} \lambda+\mu_1 & 0 & -\alpha_{31}e^{-\lambda\tau} & -\alpha_{41}e^{-\lambda\tau} & -\alpha_{51}e^{-\lambda\tau} \\ 0 & \lambda+\mu_2 & -\alpha_{32}e^{-\lambda\tau} & -\alpha_{42}e^{-\lambda\tau} & -\alpha_{52}e^{-\lambda\tau} \\ -\alpha_{13} & -\alpha_{23} & \lambda+\upsilon_1 & 0 & 0 \\ -\alpha_{14} & -\alpha_{24} & 0 & \lambda+\upsilon_2 & 0 \\ -\alpha_{15} & -\alpha_{25} & 0 & 0 & \lambda+\upsilon_3 \end{pmatrix} = 0,$$

i.e.,

$$\lambda^5 + a\lambda^4 + b\lambda^3 + c\lambda^2 + d\lambda + e + (a_1\lambda^3 + b_1\lambda^2 + c_1\lambda + d_1)e^{-\lambda\tau} + (a_2\lambda + b_2)e^{-2\lambda\tau} = 0, \quad (5)$$

where
$a = \upsilon_1 + \upsilon_2 + \upsilon_3 + \mu_2 + \mu_1$,
$b = \upsilon_1\upsilon_2 + \mu_2\upsilon_1 + \mu_2\upsilon_2 + \upsilon_3\mu_1 + \upsilon_1\upsilon_3 + \upsilon_2\upsilon_3 + \upsilon_3\mu_2 + \upsilon_1\mu_1 + \upsilon_2\mu_1 + \mu_1\mu_2$,
$c = \mu_2\upsilon_1\upsilon_2 + \upsilon_1\upsilon_3\mu_1 + \upsilon_2\upsilon_3\mu_1 + \mu_2\upsilon_3\mu_1 + \upsilon_1\upsilon_2\upsilon_3 + \upsilon_1\upsilon_3\mu_2 + \upsilon_2\upsilon_3\mu_2 + \upsilon_1\upsilon_2\mu_1 + \mu_2\upsilon_1\mu_1 + \mu_2\upsilon_2\mu_1$,
$d = \mu_2\upsilon_1\upsilon_2\upsilon_3 + \mu_2\upsilon_1\upsilon_2\mu_1 + \upsilon_1\upsilon_2\upsilon_3\mu_1 + \mu_2\upsilon_1\upsilon_3\mu_1 + \mu_2\upsilon_2\upsilon_3\mu_1$,
$e = \upsilon_3\mu_1\mu_2\upsilon_1\upsilon_2$,
$a_1 = -\alpha_{52}\alpha_{25} - \alpha_{24}\alpha_{42} - \alpha_{32}\alpha_{23} - \alpha_{31}\alpha_{13} - \alpha_{41}\alpha_{14} - \alpha_{51}\alpha_{15}$,
$b_1 = -\alpha_{52}\alpha_{25}(\upsilon_1 + \upsilon_2 + \mu_1) - \alpha_{24}\alpha_{42}(\upsilon_1 + \upsilon_3 + \mu_1) - \alpha_{32}\alpha_{23}(\upsilon_3 + \upsilon_2 + \mu_1) - \alpha_{31}\alpha_{13}(\upsilon_3 + \upsilon_2 + \mu_2) - \alpha_{41}\alpha_{14}(\upsilon_1 + \upsilon_3 + \mu_2) - \alpha_{51}\alpha_{15}(\upsilon_1 + \upsilon_2 + \mu_2)$,
$c_1 = -\alpha_{52}\alpha_{25}(\upsilon_1\upsilon_2 + \mu_1\upsilon_2 + \mu_1\upsilon_1) - \alpha_{24}\alpha_{42}(\upsilon_1\upsilon_3 + \mu_1\upsilon_3 + \mu_1\upsilon_1) - \alpha_{32}\alpha_{23}(\upsilon_3\upsilon_2 + \mu_1\upsilon_2 + \mu_1\upsilon_3) - \alpha_{31}\alpha_{13}(\upsilon_3\upsilon_2 + \mu_2\upsilon_3 + \mu_2\upsilon_2) - \alpha_{41}\alpha_{14}(\upsilon_1\upsilon_3 + \mu_2\upsilon_3 + \mu_2\upsilon_1) - \alpha_{51}\alpha_{15}(\upsilon_1\upsilon_2 + \mu_2\upsilon_1 + \mu_2\upsilon_2)$,
$d_1 = -\alpha_{52}\alpha_{25}\mu_1\upsilon_1\upsilon_2 - \alpha_{24}\alpha_{42}\mu_1\upsilon_1\upsilon_3 - \alpha_{32}\alpha_{23}\mu_1\upsilon_2\upsilon_3 - \alpha_{31}\alpha_{13}\mu_2\upsilon_2\upsilon_3 - \alpha_{41}\alpha_{14}\mu_2\upsilon_3\upsilon_1 - \alpha_{51}\alpha_{15}\mu_2\upsilon_1\upsilon_2$,

$$\begin{aligned} a_2 = {} & \alpha_{31}\alpha_{13}\alpha_{52}\alpha_{25} + \alpha_{31}\alpha_{13}\alpha_{24}\alpha_{42} - \alpha_{31}\alpha_{14}\alpha_{42}\alpha_{23} - \\ & \alpha_{31}\alpha_{15}\alpha_{52}\alpha_{23} - \alpha_{41}\alpha_{13}\alpha_{32}\alpha_{24} + \alpha_{41}\alpha_{14}\alpha_{52}\alpha_{25} + \\ & \alpha_{41}\alpha_{14}\alpha_{23}\alpha_{32} - \alpha_{41}\alpha_{15}\alpha_{52}\alpha_{42} - \alpha_{51}\alpha_{13}\alpha_{32}\alpha_{25} - \\ & \alpha_{14}\alpha_{42}\alpha_{25}\alpha_{51} + \alpha_{51}\alpha_{15}\alpha_{42}\alpha_{24} + \alpha_{51}\alpha_{15}\alpha_{23}\alpha_{32}, \end{aligned}$$

$$\begin{aligned} b_2 = {} & \alpha_{31}\alpha_{13}\alpha_{52}\alpha_{25}\upsilon_2 + \alpha_{31}\alpha_{13}\alpha_{24}\alpha_{42}\upsilon_3 - \alpha_{31}\alpha_{14}\alpha_{42}\alpha_{23}\upsilon_3 \\ & - \alpha_{31}\alpha_{15}\alpha_{52}\alpha_{23}\upsilon_2 - \alpha_{41}\alpha_{13}\alpha_{32}\alpha_{24}\upsilon_3 + \alpha_{41}\alpha_{14}\alpha_{52}\alpha_{25}\upsilon_1 \\ & + \alpha_{41}\alpha_{14}\alpha_{23}\alpha_{32}\upsilon_3 - \alpha_{41}\alpha_{15}\alpha_{52}\alpha_{42}\upsilon_1 - \alpha_{51}\alpha_{13}\alpha_{32}\alpha_{25}\upsilon_2 \\ & - \alpha_{14}\alpha_{42}\alpha_{25}\alpha_{51}\upsilon_1 + \alpha_{51}\alpha_{15}\alpha_{42}\alpha_{24}\upsilon_1 + \alpha_{51}\alpha_{15}\alpha_{23}\alpha_{32}\upsilon_2. \end{aligned}$$

To study the distribution of the roots of (5), we make the following assumption: (If we assume that $a_2 = b_2 = 0$ instead of (H2), the results in this case can be obtained from [19] analogously.)

(H2) $a_1 = b_1 = c_1 = d_1 = 0$.

Then q. (5) reduces to

$$\lambda^5 + a\lambda^4 + b\lambda^3 + c\lambda^2 + d\lambda + e + (a_2\lambda + b_2)e^{-2\lambda\tau} = 0. \tag{6}$$

Obviously, $i\omega(\omega > 0)$ is a root of q. (6) if and only if ω satisfies (the real and imaginary parts have been separated)

$$\begin{cases} -b_2 cos(2\omega\tau) - a_2\omega sin(2\omega\tau) = a\omega^4 - c\omega^2 + e, \\ -a_2\omega cos(2\omega\tau) + b_2 sin(2\omega\tau) = \omega^5 - b\omega^3 + d\omega. \end{cases} \tag{7}$$

Taking square on the both sides of the equations of (7) and summing them up, we obtain

$$\omega^{10} + (a^2 - 2b)\omega^8 + (b^2 + 2d - 2ac)\omega^6 + (c^2 + 2ae - 2bd)\omega^4 + (d^2 - 2ce - a_2^2)\omega^2 + e^2 - b_2^2 = 0. \tag{8}$$

Let $z = \omega^2$ and for convenience, denote

$$p = a^2 - 2b, q = b^2 + 2d - 2ac, r = c^2 + 2ae - 2bd, v = e^2 - b_2^2, s = d^2 - 2ce - a_2^2.$$

Then q. (8) becomes

$$z^5 + pz^4 + qz^3 + rz^2 + sz + v = 0. \tag{9}$$

Suppose that

$$h(z) = z^5 + pz^4 + qz^3 + rz^2 + sz + v.$$

The fact that q. (9) has positive roots is a necessary condition for the existence of pure imaginary roots of (6). The following four lemmas, which have been proved in [20], are going to be used to establish the distribution of positive real roots of q. (9). We should mention that the coefficients of q. (9) are different from those in Lemmas 2.1-2.4 in [20], but they have not changed the results of the lemmas. Hence, we can prove the following four lemmas analogously. So, we do not state the proofs.

emma 1. *If $v < 0$, then Eq.* (9) *has at least one positive root.*

Now, to study the distribution of positive roots of (9) when $v \geq 0$, consider the following equation that comes from $h'(z) = 0$:

$$5z^4 + 4pz^3 + 3qz^2 + 2rz + s = 0. \tag{10}$$

Substituting $z = y - \frac{p}{5}$ in q. (10), we have

$$y^4 + p_1 y^2 + q_1 y + r_1 = 0, \tag{11}$$

where $p_1 = -\frac{6}{25}p^2 + \frac{3}{5}q$, $q_1 = \frac{8}{125}p^3 + \frac{6}{25}pq + \frac{2}{5}r$, $r_1 = -\frac{3}{625}p^4 + \frac{3}{125}p^2 q - \frac{2}{25}pr + \frac{1}{5}s$. If $q_1 = 0$, then it is very easy to obtain the four roots of q. (11)

as follows:

$$y_1 = \sqrt{\frac{-p_1+\sqrt{\Delta_0}}{2}},\ y_2 = -\sqrt{\frac{-p_1+\sqrt{\Delta_0}}{2}},$$
$$y_3 = \sqrt{\frac{-p_1-\sqrt{\Delta_0}}{2}},\ y_4 = -\sqrt{\frac{-p_1-\sqrt{\Delta_0}}{2}}.$$

where $\Delta_0 = p_1^2 - 4r_1$.

emma 2. *Assume that $v \geq 0$ and $q_1 = 0$.*
(I) If $\Delta_0 < 0$, then Eq. (9) has no positive real roots.
(II) If $\Delta_0 \geq 0$, $p_1 \geq 0$ and $r_1 > 0$, then Eq. (9) has no positive real roots.
(III) If (I) and (II) are not satisfied, then Eq. (9) has positive real roots if and only if there exists at least one $z^* \in \{z_1, z_2, z_3, z_4\}$ such that $z^* > 0$ and $h(z^*) \leq 0$, where $z_i = y_i - \frac{p}{5}$ $(i = 1, 2, 3, 4)$.

Denote $p_2 = -\frac{1}{3}p_1^2 - 4r_1$, $q_2 = -\frac{2}{27}p_1^3 + \frac{8}{3}p_1 r_1 - q_1^2$, $\Delta_1 = \frac{1}{27}p_2^3 + \frac{1}{4}q_2^2$,

$$s_* = \sqrt[3]{-\frac{q_2}{2}+\sqrt{\Delta_1}} + \sqrt[3]{-\frac{q_2}{2}-\sqrt{\Delta_1}} + \frac{1}{3}p_1,\ \Delta_2 = -s_* - p_1 + \frac{2q_1}{\sqrt{s_*-p_1}}$$

and $\Delta_3 = -s_* - p_1 - \frac{2q_1}{\sqrt{s_*-p_1}}$.

emma 3. *Suppose that $v \geq 0$, $q_1 \neq 0$ and $s_* > p_1$.*
(I) If $\Delta_2 < 0$ and $\Delta_3 < 0$, then Eq. (9) has no positive real roots.
(II) If (I) is not satisfied, then Eq. (9) has positive real roots if and only if there exists at least one $z^* \in \{z_1, z_2, z_3, z_4\}$ such that $z^* > 0$ and $h(z^*) \leq 0$, where $y_1 = \frac{-\sqrt{s_*-p_1}+\sqrt{\Delta_2}}{2}$, $y_2 = \frac{-\sqrt{s_*-p_1}-\sqrt{\Delta_2}}{2}$, $y_3 = \frac{\sqrt{s_*-p_1}+\sqrt{\Delta_3}}{2}$, $y_4 = \frac{\sqrt{s_*-p_1}-\sqrt{\Delta_3}}{2}$ and $z_i = y_i - \frac{p}{5}$ $(i = 1, 2, 3, 4)$.

emma 4. *Assume that $v \geq 0$, $q_1 \neq 0$ and $s_* < p_1$, then Eq. (9) has positive real roots if and only if $\frac{q_1^2}{4(p_1-s_*)^2} + \frac{s_*}{2} = 0$, $\bar{z} > 0$ and $h(\bar{z}) \leq 0$, where $\bar{z} = \frac{q_1}{2(p_1-s_*)} - \frac{1}{5}p$.*

Suppose that q. (9) has positive roots and without loss of generality, we assume that it has five positive roots, denoted by z_k^*, $k = 1, 2, 3, 4, 5$. Then q. (8) has five positive roots $\omega_k = \sqrt{z_k^*}$, $k = 1, 2, 3, 4, 5$.

By q. (7), we have:

$$cos(2\omega_k\tau) = \frac{a_2\omega_k^6 + (ab_2 - a_2b)\omega_k^4 + (da_2 - cb_2)\omega_k^2 + eb_2}{-b_2^2 - a_2^2\omega_k^2},$$

$$sin(2\omega_k\tau) = \frac{(b_2 - aa_2)\omega_k^5 + (ca_2 - bb_2)\omega_k^3 + (db_2 - ea_2)\omega_k}{a_2^2\omega_k^2 + b_2^2}.$$

Thus, we get the corresponding $\tau_k^{(j)} > 0$ such that the characteristic equation (6) has purely imaginary roots.

$$\tau_k^{(j)} = \frac{1}{2\omega_k}[cos^{-1}(-\frac{a_2\omega_k^6 + (ab_2 - a_2b)\omega_k^4 + (da_2 - cb_2)\omega_k^2 + eb_2}{b_2^2 + a_2^2\omega_k^2}) + 2j\pi], \tag{12}$$

where $k = 1, 2, 3, 4, 5$ and $j = 0, 1, 2, \ldots$, then $\pm i\omega_k$ is a pair of purely imaginary roots of q. (6) with $\tau = \tau_k^{(j)}$. Clearly, the sequence $\{\tau_k^{(j)}\}_{j=0}^{+\infty}$ is increasing, and $lim_{j\to+\infty}\tau_k^{(j)} = +\infty$, $k = 1, 2, 3, 4, 5$.

Therefore, we can define

$$\tau_0 = \tau_{k_0}^{(0)} = min_{k\in\{1,\ldots,5\}}\{\tau_k^{(0)}\},\ \omega_0 = \omega_{k_0},\ z_0 = z_{k_0}^*. \tag{13}$$

For convenience, we make the following hypotheses:

(H3) $a > 0$, $ab - c > 0$, $c(ab - c) + a(e + b_2 - a(d + a_2)) > 0$, $e + b_2 > 0$
$(ab - c)[c(d + a_2) - b(e + b_2)] - [a(d + a_2) - e - b_2]^2 > 0$.

We also need the following result from Ruan and Wei [22].

emma . *Consider the exponential polynomial*

$$\begin{aligned} P(\lambda, e^{-\lambda\tau_1}, \ldots, e^{-\lambda\tau_m}) &= \lambda^n + p_1^{(0)}\lambda^{n-1} + \ldots + p_{n-1}^{(0)}\lambda + p_n^{(0)} \\ &+ [p_1^{(1)}\lambda^{n-1} + \ldots + p_{n-1}^{(1)}\lambda + p_n^{(1)}]e^{-\lambda\tau_1} + \ldots \\ &+ [p_1^{(m)}\lambda^{n-1} + \ldots + p_{n-1}^{(m)}\lambda + p_n^{(m)}]e^{-\lambda\tau_m}, \end{aligned}$$

where $\tau_i \geq 0\,(i = 1, 2, \ldots, m)$ and $p_j^{(i)}$ $(i = 0, 1, 2, \ldots, m; j = 1, 2, \ldots, n)$ are constants. As $(\tau_1, \tau_2, \ldots, \tau_m)$ vary, the sum of the orders of the zeros of $P(\lambda, e^{-\lambda\tau_1}, \ldots, e^{-\lambda\tau_m})$ on the open right half plane can change only if a zero appears on or crosses the imaginary axis.

Proof. See [22]. □

Using Lemmas 1-5, we can easily obtain the following results on the distribution of roots of the q. (6).

emma 6. *Assume that (H3) holds.*
(I) If one of the following conditions holds:
(a) $v < 0$;
(b) $v \geq 0$, $q_1 = 0$, $\Delta_0 \geq 0$ and $p_1 < 0$ or $r_1 \leq 0$ and there exists $z^* \in \{z_1, z_2, z_3, z_4\}$ such that $z^* > 0$ and $h(z^*) \leq 0$;
(c) $v \geq 0$, $q_1 \neq 0$, $s_* > p_1$, $\Delta_2 \geq 0$ or $\Delta_3 \geq 0$ and there exists $z^* \in \{z_1, z_2, z_3, z_4\}$ such that $z^* > 0$ and $h(z^*) \leq 0$;
(d) $v \geq 0$, $q_1 \neq 0$, $s_* < p_1$, $\frac{q_1^2}{4(p_1 - s_*)^2} + \frac{1}{2}s_* = 0$, $\bar{z} > 0$ and $h(\bar{z}) \leq 0$,
then all roots of Eq. (6) have negative real parts when $\tau \in [0, \tau_0)$.

(II) If none of the conditions (a)-(d) of (I) is satisfied, then all roots of Eq. (6) *have negative real parts for all* $\tau \geq 0$.

Proof. When $\tau = 0$, q. (6) becomes

$$\lambda^5 + a\lambda^4 + b\lambda^3 + c\lambda^2 + (d + a_2)\lambda + e + b_2 = 0. \tag{14}$$

By the Routh-Hurwitz criterion, all roots of q. (14) have negative real parts if and only if (H3) holds. From Lemmas 1-4, we know that if (a)-(d) of (I) are not satisfied, then q. (6) has no roots with zero real part for all $\tau \geq 0$. If one of (a)-(d) holds, when $\tau \neq \tau_k^{(j)}$, $k = 1, \ldots, 5$; $j = 0, 1, \ldots$, q. (6) has no roots with zero real part and τ_0 is the minimum value of τ so that q. (6) has purely imaginary roots. Applying Lemma 5, we obtain the conclusion of the lemma. □

Let

$$\lambda(\tau) = \alpha(\tau) + i\omega(\tau) \tag{15}$$

be the root of q. (6) satisfying $\alpha(\tau_0) = 0$, $\omega(\tau_0) = \omega_0$. Then we have the following lemma:

emma 7. *Suppose that* $z_0 = \omega_0^2$, $h'(z_0) \neq 0$ *and* $a_2\omega_0 \neq 0$ *(or* $b_2 \neq 0$*). Then, at* $\tau = \tau_0$, $\pm i\omega_0$ *is a pair of simple purely imaginary roots of Eq.* (6)*. Moreover,*

$$\frac{dRe(\lambda(\tau_0))}{d\tau} \neq 0,$$

also, $\frac{dRe(\lambda(\tau_0))}{d\tau}$ *and* $h'(z_0)$ *have the same sign.*

Proof. Differentiating q. (6) with respect to τ, we can easily obtain:

$$[\frac{d\lambda}{d\tau}]^{-1} = \frac{(5\lambda^4 + 4a\lambda^3 + 3b\lambda^2 + 2c\lambda + d)e^{2\lambda\tau} + a_2}{2a_2\lambda^2 + 2b_2\lambda} - \frac{\tau}{\lambda}.$$

Then, we get

$$[\frac{dRe(\lambda(\tau_0))}{d\tau}]^{-1} = \frac{z_0}{K}h'(z_0),$$

where $K = 4a_2^2\omega_0^4 + 4b_2^2\omega_0^2$. Thus, we obtain

$$sign\{\frac{dRe(\lambda(\tau_0))}{d\tau}\} = sign\{[\frac{dRe(\lambda(\tau_0))}{d\tau}]^{-1}\} = sign\{\frac{z_0}{K}h'(z_0)\} \neq 0.$$

Since $K, z_0 > 0$, we conclude that the sign of $\frac{dRe(\lambda(\tau_0))}{d\tau}$ is determined by the sign of $h'(z_0)$. □

Now, we state the main theorem:

Theorem 1. *Suppose that (H1), (H2) and (H3) hold.*
(I) If the conditions (a)-(d) of Lemma 6 are all not satisfied, then the zero

solution of system (3) *is asymptotically stable for all* $\tau \geq 0$.
(II) If one of the conditions (a)-(d) of Lemma 6 is satisfied, then the zero solution of system (3) *is asymptotically stable for all* $\tau \in [0, \tau_0)$.
(III) If all the conditions as stated in (II) hold and $h'(z_0) \neq 0$, *then system* (3) *undergoes a Hopf bifurcation at the zero solution as* τ *passes through* τ_0.

Proof. By applying Lemmas 6, 7 and bifurcation theory, all parts can be easily proved. □

(For more information about bifurcation theory and Hopf bifurcation, see [23].)

3 Numerical simulation

In this section, we give a numerical simulation to support our theoretical analysis. We consider the following system

$$\begin{cases} \dot{x_1}(t) = -0.5x_1(t) + tanh(y_1(t-\tau_2)) \\ \qquad\quad -tanh(y_2(t-\tau_2)) + 2tanh(y_3(t-\tau_2)) \\ \dot{x_2}(t) = -x_2(t) + tanh(y_1(t-\tau_2)) \\ \qquad\quad +tanh(y_2(t-\tau_2)) + tanh(y_3(t-\tau_2)) \\ \dot{y_1}(t) = -2y_1(t) + tanh(x_1(t-\tau_1)) - tanh(x_2(t-\tau_1)) \\ \dot{y_2}(t) = -0.5y_2(t) + tanh(x_1(t-\tau_1)) + tanh(x_2(t-\tau_1)) \\ \dot{y_3}(t) = -0.5y_3(t) + tanh(x_1(t-\tau_1)) - tanh(x_2(t-\tau_1)) \end{cases} \tag{16}$$

which has $(0,0,0,0,0)$ as an equilibrium point. From section 2, by (5) and (8), we can compute $p = 9$, $q = 27.375$, $r = 32.3125$, $s = -24.43359375$ and $v = -0.984375$. Then q. (9) has a unique positive real root $z_0 = 0.5308$. Its easy to show that $\tau_0 = 0.885959203$, $h'(z_0) > 0$ and $sign\{\frac{d(Re\lambda(\tau_0))}{d\tau}\} = 1$. Here, we have chosen $\tau_1 = 0.3$ and $\tau_2 = 0.4$, Figure 1 shows that the origin is asymptotically stable. When τ passes through the critical value τ_0, a Hopf bifurcation occurs and a family of stable periodic solutions bifurcates from the origin. In Figure 2, the bifurcating periodic solutions are presented by choosing $\tau_1 = 0.4$ and $\tau_2 = 0.5$.

4 Conclusions

In this paper, we discussed the dynamics of a class of BAM neural network with two neurons in the X-layer, three neurons in the Y-layer and two time delays. We have proved that the zero solution loses its stability and Hopf bifurcation occurs. In fact, a family of periodic solutions bifurcate from the zero solution when τ passes through a critical value. Also, in the main

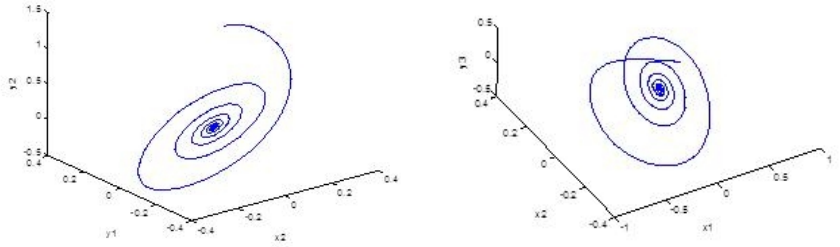

Figure 1: When $\tau_1 = 0.3$ and $\tau_2 = 0.4$, the origin is asymptotically stable.

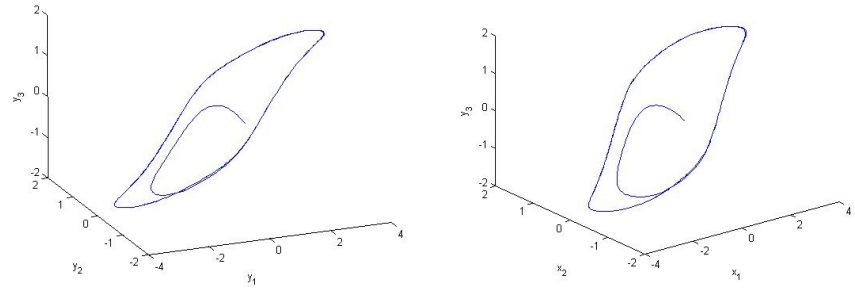

Figure 2: When $\tau_1 = 0.4$ and $\tau_2 = 0.5$, a family of periodic solutions bifurcates from the origin.

theorem, we resulted asymptotically stability of the zero solution in system (3) under some conditions. Finally, the results have been illustrated through numerical simulations.

At the end, for further research, we would like to point out that we discussed the dynamics of a special class of BAM neural network, but the complexity found in this case might be carried out to larger networks under some conditions.

References

1. Hopfield, J. J. *Neurons with graded response have collective computational properties like those of two-state neurons.* Proc. Nat. Acad. Sci. USA, 81 (1984), 3088–3092.

2. Marcus, C. M. and Westervelt, R. M. *Stability of analog neural network with delay.* Phys. Rev. A, 39 (1989), 347–359.

3. Cao, J. and Wang, J. *Absolute exponential stability of recurrent neural networks with Lipschitz continuous activation and time delays.* Neural Networks, 17 (2004), 379–390.

4. Cao, J. D. and Zhou, D. *Stability analysis of delayed cellular neural networks.* Neural Networks, 11 (1998), 1601–1605.

5. Guo, S. and Huang, L. *Hopf bifurcating periodic orbits in a ring of neurons with delays.* Physica D, 183 (2003), 19–44.

6. Hu, H. and Huang, L. *Stability and Hopf bifurcation analysis on a ring of four neurons with delays.* Applied Mathematics and Computation, 213 (2009), 587–599.

7. Liao, X., Wong, . and Wu, Z. *Bifurcation analysis on a two-neuron system with distributed delays.* Physica D, 149 (2001), 123–141.

8. Li, Y., Chen, X. and Zhao, L. *Stability and existence of periodic solution to delayed Cohen-Grossberg BAM neural networks with impulses on time scales.* Neurocomputing, 72 (2009), 1621–1630.

9. Liu, X., Martin, R. R., Wu, M. and Tang, M. *Global exponential stability of bidirectional associative memory neural networks with time delays.* I Trans. Neural Network, 19 (3) (2008), 397–407.

10. Xu, C., He, X. and Li, P. *Global existence of periodic solutions in a six-neuron BAM neural network model with discrete delays.* Neurocomputing, 74 (2011), 3257–3267.

11. osko, B. *Adaptive bidirectional associative memories.* Appl. Opt., 26 (1987), 4947–4960.

12. Gopalsamy, . and He, X. *Delay-independent stability in bi-directional associative memory networks.* I Trans. Neural Networks, 5 (1994), 998–1002.

13. Cao, J. and Xiao, M. *Stability and Hopf bifurcation in a simplified BAM neural network with two time delays.* I Transaction on Neural Networks, 18 (2007), 416–430.

14. Ge, J. and Xu, J. *Synchronization and synchronized periodic solution in a simplified five-neuron BAM neural network with delays.* Neurocomputing, 74 (2011), 993–999.

15. Li, C., Liao, X. and Zhang, R. *Delay-dependent exponential stability analysis of bi-directional associative memory neural networks with time delay: an LMT approach.* Chaos Solitons Fractals, 24 (2005), 1119–1134.

16. Song, Y., Han, M. and Wei, J. *Stability and Hopf bifurcation analysis on a simplified BAM neural network with delays.* Physica D, 200 (2005), 185–204.

17. Sun, C. and Han, M. *Global Hopf bifurcation analysis on a BAM neural network with delays.* Math. Comput. Modelling, 45 (2007), 61–67.

18. Xu, C. J., Tang, X. H. and Liao, M. X. *Frequency domain analysis for bifurcation in a simplified tri-neuron BAM network model with two delays.* Neural Networks, 23 (2010), 872–880.

19. Yang, Y. and Ye, J. *Stability and bifurcation in a simplified five-neuron BAM neural network with delays.* Chaos, Solitons and Fractals, 42 (2009), 2357–2363.

20. Zhang, T., Jiang, H. and Teng, Z. *On the distribution of the roots of a fifth degree exponential polynomial with application to a delayed neural network model.* Neurocomputing, 72 (2009), 1098–1104.

21. Javidmanesh, ., Afsharnezhad, Z. and ffati, S. *Existence and stability analysis of bifurcating periodic solutions in a delayed five-neuron BAM neural network model.* Nonlinear Dyn. 72 (2013), 149–164.

22. Ruan, S. and Wei, J. *On the zeros of transcendental functions with applications to stability of delay differential equations with two delays.* Dynamics of Continuous Discrete and Impulsive Systems Series A: Mathematics and Analytical 10 (2003), 863–874.

23. Hassard, B. D., azarinoff, N. D. and Wan, Y. H. *Theory and applications of Hopf bifurcation.* Cambridge University Press, Cambridge (1981).

Iranian J. of Numerical Anal sis and Optimization
Vol 3, No. 2, 2013 , pp 13-20

Optimization of electron Raman scattering in double rectangular quantum wells

A. eshavarz and N. Zamani

Abstract

In this ork, b using the particle s arm optimization the electron Raman scattering for s uare double uantum ells is optimized. For this purpose, b combining the particle s arm algorithm together ith the numerical solution procedures for e uations, and also the perturbation theor e find the optimal structure that maximizes the electron Raman scattering. Application of this algorithm to the structure of as mmetric double uantum ells sho s that the differential cross section of an electron Raman scattering is $1.30390 \times 10^5 Arb.Units$.

ey ords: Particle swarm optimization; lectron Raman scattering; Asymmetric double quantum wells.

1 Introduction

The possibility of nanofabrication of new electro-optical devices based in low-dimensional systems has led to enormous interest in the investigation of semiconductor nanostructures such as: quantum wells, quantum dots, supperlattices and quantum wires, which are usually made with epitaxially grown materials (for instance $GaAs/AlAs$). In recent years, there has been considerable interest in double quantum well systems; because many new optical devices based on intersubband transitions are being developed. This feature could full the need for efcient sources of coherent mid-infrared radiation for application in several branches of science and technology, such as communications, radar, optical electronics. For example, an intersubband Raman laser can be built with a three-level system[1, 3, 2]. In an asymmetric double quantum well (ASDQW) structure, which consists of two different width wells

Recieved 27 August 2012; accepted 27 Ma 2013
A. Keshavarz
Department of h sics, ollege of Science, Shiraz niversit of Technolog , *313-71555*, Shiraz, Iran. e-mail keshavarz sutech.ac.ir

N. Zamani
Department of h sics, ollege of Science, Shiraz niversit of Technolog , *313-71555*, Shiraz, Iran. e-mail n.zamani sutech.ac.ir

coupled with a thin barrier, the system consists of two GaAs wells separated by AlxGa1-xAs barriers.

Raman scattering experiments are well known to provide a powerful technique for the investigation of direct physical properties of semiconductor nanostructures[8, 7]. The electronic structure of nanostructures and other materials can be studied through the use of Raman scattering processes considering different polarizations of incident and emitted radiation[4, 5]. In all previous work, studies show that the RS of nanostructure are strongly affected by the material and impurities, geometrical and as well as the external factors such as electric and magnetic elds[6, 9, 10, 11]. Studying in this matter is based on the investigation of the effective parameters in the RS of those nanostructures. This property can be modified and controlled by tuning the geometrical parameters such as barrier width and the well width which in double quantum well contains ve parameters as shown in Fig.1. In all of the previous works the sensitivity of the RS for one of these parameters is investigated separately, but the effect of all parameters have not been discussed simultaneously. In the present work, we optimize the RS with intersubband transitions within the conduction band for ASDQW. For this purpose, we calculate the energy eigenvalues and eigenfunctions of the system and then by using the particle swarm optimization(PSO) method and the variation of different values of the well parameter we obtain the optimum structure for maximized RS.

2 Theory

The problem of finding the bound states of an electron in the envelope function approximation for a semiconductor ASDQW systems of rectangular form (grown along the z-direction), leads us to solving the Schrödinger equation with constant mass m^* is given by:

$$\left(-\frac{\hbar^2}{2m^*}\frac{d^2}{dx^2}+V(z)\right)\psi(z)=E\psi(z), \tag{1}$$

where the one-dimensional $V(z)$ is potential profile of the ASDQWs and introduced mathematically as:

$$V(z)=\begin{cases} V_0 \; z\leq -(L_l+\frac{L_b}{2}), \\ 0 \; -(L_l+\frac{L_b}{2})<z<-(\frac{L_b}{2}), \\ V_0 \; -(\frac{L_b}{2})\leq z\leq (\frac{L_b}{2}), \\ V_1 \; (\frac{L_b}{2})<z<(L_r+\frac{L_b}{2}), \\ V_0 \; z\geq (L_r+\frac{L_b}{2}) \end{cases} \tag{2}$$

Fig.1 shows the schematic illustration for this structure where b is the $Al_xGa_{1-x}As$ barrier thickness, L_l and L_r are the left and right $GaAs$ quantum well thickness, respectively. By using the numerical method one can be obtained the energy levels and corresponding wave function for electrons in conduction band of ASDQW.

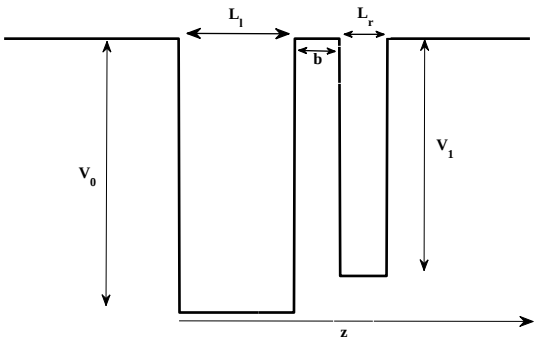

Figure 1: Schematic diagram for an asymmetric double quantum wells.

After the energies and their corresponding wave functions are obtained, can be used to calculate the RS that the general expression for the RS differential cross-section is given by[12]

$$\frac{d^2\sigma}{d\omega_s d\Omega} = \frac{V^2\omega_s^2 n(\omega_s)}{8\pi^3 c^4 n(\omega_l)} W(\omega_s, \mathbf{e}_s), \tag{3}$$

where c is the velocity of light in vacuum, $n(\omega)$ is the refractive index as a function of the radiation frequency, $\mathbf{e}_s(\mathbf{e}_l)$ is the polarization vector for the emitted secondary radiation field, ω_s is the secondary radiation frequency, ω_l is the frequency of the incident radiation. $W(\omega_s, \mathbf{e}_s)$ is the transition rate for the secondary radiation and calculated in perturbation theory and substituting in q.35 the differential cross-section for a three-level system for ASDQW is expressed in the form of[13]:

$$\left[\frac{d^2\sigma}{d\Omega d\omega_s}\right]_i = \sigma_0 \frac{\omega_s}{\omega_l} |M_0(i)|^2 \frac{E_0^2}{[\hbar\omega_l - \hbar\omega_s + E_1 - E_2]^2 + \Gamma_f^2}, \tag{4}$$

where $M_0(i) = E_0 \frac{T_{2,3}(i)T_{3,1}(i)}{\hbar\omega_s + E_2 - E_3 + i\Gamma_a}$, $\sigma_0 = \frac{4e^4 n(\omega_s)\hbar\Gamma_f}{\pi m_0^{*2} c^4 n(\omega_l) E_0^2} |(\mathbf{e}_l \cdot \mathbf{e}_z)(\mathbf{e}_s \cdot \mathbf{e}_z)|^2$ and $E_0 = \frac{\hbar^2}{2m_0^* d_r^2}$. In this paper, a PSO is used to optimize the ASQWs structure in order to maximize the RS. The PSO is a modern heuristic algorithm based on the social behaviour of bird flocks, colonies of insects, schools of shes, and groups of animals feeding and travelling together. This algorithm

was first introduced by ennedy and berhat[14]which has now been widely used in function optimization applicable in mathematics and physics. The algorithm is started by initializing a population of random solutions called particles and searches for the best position by updating production through the following velocity and position update equations. The velocity and position are updated by the following equations:

$$Vel_j^{t+1} = \omega \times Vel_j^t + c_1 \times rand_1(.) \times (Pbest_j - X_j^t) + c_2 \times rand_2(.) \times (Gbest - X_j^t), \quad (5)$$

$$X_j^{t+1} = X_j^t + Vel_j^{t+1}, \quad (6)$$

$$\omega^{t+1} = \omega_{max} - \frac{\omega_{max} - \omega_{min}}{t_{max}} \times t, \quad (7)$$

where $j = 1, 2, ..., N_{Swarm}$ is the index of each particle, N_{Swarm} is the number of the swarms, t is the current iteration number, $rand_1(.)$ and $rand_2(.)$ are random numbers between 0 and 1. Vel_j^t is the current velocity of particle j at iteration t, Vel_j^{t+1} is the modified velocity of particle j at iteration $t+1$, X_j^t is the current position of particle j at iteration t, $Pbest_j$ is the optimal coordinate value of the jth particle obtained so far and $Gbest$ is the best coordinate value found so far in the whole swarm. Constants c_1 and c_2 are the weighting factors of the stochastic acceleration terms, which pull each particle towards the $Pbest_j$ and $Gbest$. ω is a non-negative constant called inertia weight and used to control the convergence behaviour of the PSO. Here the position of particle involves width of two wells and barrier and height for two wells.

3 Numerical solution and disscussion

Considering RS of the ASDQW is strongly affected by the geometrical size and any changes in the structure leads to changes in the RS and the frequency of the secondary radiation. Using the above optimization algorithm, we determine the optimal structure parameters for maximized RS. In order to use the PSO algorithm, minimum amounts in which there are three energy levels for quantum wells are obtained. The materil parameters used in this paper are as follows: $m^*_{GaAs} = 0.067m_0$, $m^* = 0.067m_0$, $m^*_{AlGaAs} = 0.067m_0$, $m^* = (0.067 + 0.083x)m_0$ where m_0 is the mass of the free electron, incident radiation energy $\hbar\omega_l = 230(meV)$ and the lifetimes of the final and intermediate states are given as $\Gamma_a = \Gamma_f = 3(meV)$, respectively. The rang of particles in the width and height of two wells which are separated by a barrier are given as: $L_l \in [50, 90]A^\circ$, $L_r \in [20, 60]A^\circ$, $b \in [15, 30]A^\circ$, $V_0 \in [300, 400](meV)$ and $V_1 \in [300, 400](meV)$. Results obtained using the PSO algorithm are shown

Table 1: Result of PSO

$L_l(A^\circ)$	$L_r(A^\circ)$	$b(A^\circ)$	$V_0(meV)$	$V_1(meV)$
60	30	15	390	390

in Table.1.

As the PSO algorithm is a random statistical algorithm, the typical convergence plots of PSO for nding optimal absorption for 50 iterations is shown in Fig.2. In this figure shows that by using the PSO algorithm after 20 iteration optical rectification coefficient has a constant value which is equal to $1.30390 \times 10^5 Arb.Units$.

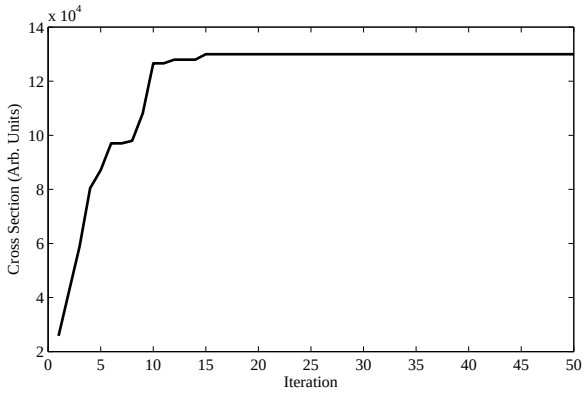

Figure 2: Convergence plot of PSO for nding optimal RS.

The optimum structure of double quantum wells depicts in Fig.3. includes the wave functions of ASDQWs. Seen that optimum structure is asymmetric and using the numerical solutions.

Fig.4 display the RS as a function of secondary radiation photon energy $\hbar\omega_s$ for our optimal structure. This indicates that resonant peak at photon energy value of $125.498\,(meV)$ as expected corresponding to the is $\hbar\omega_s = E3 - E2$ and non-resonant peak at photon energy value of $125.473\,(meV)$ as expected corresponding to the is $\hbar\omega_s = \hbar\omega_l + E3 - E2$. From this figure we see that resonant and non-resonant are overlapping and the magnitude of the non-resonant peak is $1.30390 \times 10^5 Arb.Units$. We should note that the resonant peak does not depend on incoming radiation and the non-resonant peak depends on it.

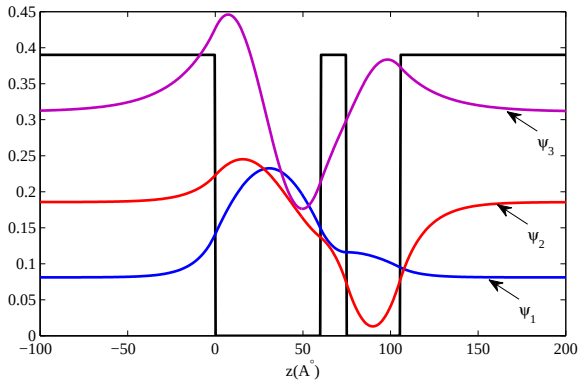

Figure 3: Schematic diagram for an asymmetric double quantum well for optimal parameters with wave function.

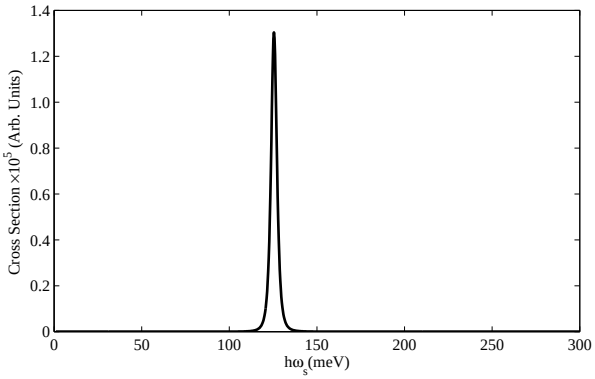

Figure 4: Schematic diagram for an asymmetric double quantum well for optimal parameters with wave function.

4 Conclusion

The RS of quantum wells which depend on the energy eigenstate and their corresponding eigenfunctions associate with the potential shape and geometrical features are calculated numerical by solving the equation. The calculations mainly focus we to find the optimum parameters to maximize the RS. For this purpose we used the particle swarm optimization and introduce the geometrical set of parameters.

Acknowledgements

The authors would like to express their special gratitude to the Shiraz University of Technology.

References

1. Betancourt-Riera, R., Riera, R. and Rosas, R. *Electron Raman scattering in asymmetrical multiple quantum wells system with an external electric field.* Physica : Low-dimensional Systems and Nanostructures, 44 (2012), 1152–1157.

2. Betancourt-Riera, R., Rosas, R., Marn- nriquez, I., Riera, R. and Marin, J. L. *Electron Raman scattering in asymmetrical multiple quantum wells.* Journal of Physics: Condensed Matter, 17 (2005), 4451–4461.

3. Cardona, M. *Lattice vibrations in semiconductor superlattices.* Superlattices and microstructures, 7 (1990), 183–192.

4. Cardona, M. and Guntherodt, G. *Light Scattering in Solids V (Topics in Applied Physics 66)*, Springer, Heidelberg, 1989.

5. Comas, F., Trallero-Giner, C. and Perez-Alvarez, R. *Interband-intraband electronic Raman scattering in semiconductors.* Journal of Physics C: Solid State Physics, 19 (1986), 6479–6488.

6. Ismailov, T. G. and Mehdiyev, B. H. *Electron Raman scattering in a cylindrical quantum dot in a magnetic field.* Physica : Low-dimensional Systems and Nanostructures, 31 (2006), 72–77.

7. ennedy, J. and berhart, R. *Particle swarm optimization.* In Neural Networks, 1995. Proceedings., I International Conference on, 4 (1995), 1942–1948.

8. hurgin, J. B., Sun, G., Friedman, L. R. and Soref, R. A. *Comparative analysis of optically pumped intersubband lasers and intersubband Raman oscillators.* Journal of applied physics, 78 (1995), 7398–7400.

9. lein, M. *Phonons in semiconductor superlattices.* I Journal of Quantum lectronics, 22 (1986), 1760-1770.

10. Liu, A. and Ning, C. Z. *Terahertz optical gain based on intersubband transitions in optically pumped semiconductor quantum wells: Coherent pumpprobe interactions.* Applied physics letters, 75 (1999), 1207–1209.

11. Riera, R., Comas, F., Trallero Giner, C. and Pavlov, S. T. *Electron Raman scattering in semiconductor quantum wells.* physica status solidi (b), 148 (1988), 533–542.

12. Sun, G., hurgin, J. B., Friedman, L. R. and Soref, R. A. *Tunable intersubband Raman laser in GaAs/AlGaAs multiple quantum wells.* JOSA B, 15 (1998), 648–651.

13. Xie, W. *Electron Raman scattering of a two-dimensional pseudodot system.* Physics Letters A, 376 (2012), 1660–1657.

14. Zhao, X. and Liu, C. *"One-phonon resonant Raman scattering in cylindrical quantum wires.* Physica : Low-dimensional Systems and Nanostructures, 36 (2007), 34–39.

Iranian J. of Numerical Anal sis and Optimization
Vol 3, No. 2, 2013 , pp 21-31

Approximate Analytical Solution for Quadratic Riccati Differential Equation

H. Aminikhah

Abstract

In this paper, e introduce an efficient method for solving the uadratic Riccati differential e uation. In this techni ue, combination of Laplace transform and ne homotop perturbation methods LTNH M are considered as an algorithm to the exact solution of the nonlinear Riccati e uation. n-like the previous approach for this problem, so-called NH M, the present method, does not need the initial approximation to be defined as a po er series. Four examples in different cases are given to demonstrate simplicit and efficienc of the proposed method.

ey ords: Riccati differential equation; Laplace transform method; NHPM; LTNHPM.

1 Introduction

The quadraic Riccati differential equation, deriving its name from Jacopo Francesco, Count Riccati (1676-1754). These kinds of differential equations are a class of nonlinear differential equations of much importance, and play a significant role in many fields of applied science [1]. At an early stage, the occurrence of such differential equations in the study of Bessel functions led to its appearance in many related applications and, to the present time, the literature on the Riccati equation has been extensive. For several reasons, a Riccati equation comprises of a highly significant class of nonlinear ordinary differential equations. Firstly, this equation is closely related to ordinary linear homogeneous differential equation of the second order. Secondly, the solution of Riccati equation possesses a very particular structure in that the general solution is a fractional linear function of the constant of integration. Thirdly, the solution of an Ricaati equation is involved in the reduction of nth-order linear homogeneous ordinary differential equations. Fourthly, a one-dimensional Schrodinger equation is closely related to Riccati differential

Recieved 18 Februar 2013; accepted 12 June 2013
H. Aminikhah
Department of Applied Mathematics, School of Mathematical Sciences, niversit of Guilan, .O. Box 1914, Rasht, Iran.
e-mail aminikhah guilan.ac.ir

equation. Solitary wave solutions of a nonlinear partial differential equation can be expressed as a polynomial in two elementary functions satisfying a projective Riccati equation [3]. Moreover, such types of problems also arise in the optimal control literature, and can be derived in solving a second-order linear ordinary differential equation with constant coefficients [2]. In conformity with the general study of differential equations, much of the early works were concerned with the study of particular classes of Riccati differential equation with the aim of determining the solution in finite form. Many mathematicians such as Jame Bernouli, Jahn Bernouli (1667-1748), Leonhard uler (1707-1783), Jean-le-Rondd'Alembert(1717-1783), and Adrian Marine Legendre (1752-1833) contributed to the study of such differential equations [1]. Deriving analytical solution for Riccati equation in an explicit form seems to be unlikely except for certain special situations. Of course, having known its one particular solution, its general solution can be easily derived. Therefore, one has to go for numerical techniques or approximate approaches for getting its solution. Recently, Adomian's decomposition method has been proposed for solving Riccati differential equations [7, 8]. HPM was introduced by He [4] and has been already used by many mathematicians and engineers to solve various functional equations [9, 10, 5, 6, 12, 11]. Abbasbandy solved a Riccati differential equation using He's VIM, homotopy perturbation method (HPM) and iterated He's HPM and compared the accuracy of the obtained solution to that derived by Adomian decomposition method [13, 14, 16]. Moreover, Homotopy analysis method (HAM) and a piecewise variational iteration method (VIM) are proposed for solving Riccati differential equations [16]. In [15], Liao has shown that HPM equations are equivalent to HAM equations when $\hbar = -1$. Aminikhah and Hemmatnezhad [6] proposed a new homotopy perturbation method (NHPM) to obtain the approximate solution of ordinary Riccati differential equation. In this work, we present the solution of Riccati equation by combination of placeLaplace transform and new homotopy perturbation methods. An important property of the proposed method, which is clearly demonstrated in examples, is that spectral accuracy is accessible in solving specific nonlinear Riccati differential equations which have analytic solution functions.

2 LTNHPM for quadratic Ricatti equation

Consider the nonlinear Riccati differential equation as the following form

$$\begin{cases} u'(t) = A(t) + B(t)u(t) + C(t)u^2(t), \ 0 \le t \le T, \\ u(0) = \alpha. \end{cases} \tag{1}$$

where $A(t)$, $B(t)$ and $C(t)$ are continuous and α is an arbitrary constant. By the new homotopy technique, we construct a homotopy $U : \Omega \times [0, 1] \to \mathbb{R}$,

which satisfies

$$H(U(t),p) = U'(t) - u_0(t) + pu_0(t) - p[A(t) + B(t)U(t) + C(t)U^2(t)] = 0, \quad (2)$$

where $p \in [0,1]$ is an embedding parameter, $u_0(t)$ is an initial approximation of solution of equation (1). Clearly, we have from equation (2)

$$H(U(t),0) = U'(t) - u_0(t) = 0, \quad (3)$$

$$H(U(t),1) = U'(t) - A(t) - B(t)U(t) - C(t)U^2(t) = 0 \quad (4)$$

By applying Laplace transform on both sides of (2), we have

$$\mathrm{L}\left\{U'(t) - u_0(t) + pu_0(t) - p[A(t) + B(t)U(t) + C(t)U^2(t)]\right\} = 0 \quad (5)$$

Using the differential property of Laplace transform we have

$$s\mathrm{L}\{U(t)\} - U(0) = \mathrm{L}\left\{u_0(t) - pu_0(t) + p[A(t) + B(t)U(t) + C(t)U^2(t)]\right\} \quad (6)$$

or

$$\mathrm{L}\{U(t)\} = \frac{1}{s}\left\{U(0) + \mathrm{L}\left\{u_0(t) - pu_0(t) + p[A(t) + B(t)U(t) + C(t)U^2(t)]\right\}\right\} \quad (7)$$

By applying inverse Laplace transform on both sides of (7), we have

$$U(t) = \mathrm{L}^{-1}\{\frac{1}{s}\{U(0) + \mathrm{L}\{u_0(t) - pu_0(t) + p[A(t) + B(t)U(t) + C(t)U^2(t)]\}\}\} \quad (8)$$

According to the HPM, we use the embedding parameter p as a small parameter, and assume that the solutions of equation (8) can be represented as a power series in p as $U(t) = \sum_{n=0}^{\infty} p^n U_n$. Now let us write the q. (8) in the following form

$$\sum_{n=0}^{\infty} p^n U_n(t) = \mathrm{L}^{-1}\left\{\frac{1}{s}\Big(U(0) + \mathrm{L}\Big\{u_0(t) - pu_0(t) + p\Big[A(t) + B(t)\sum_{n=0}^{\infty} p^n U_n(t) + C(t)(\sum_{n=0}^{\infty} p^n U_n(t))^2\Big]\Big\}\Big)\right\} \quad (9)$$

Comparing coefficients of terms with identical powers of p leads to

$$\begin{aligned} p^0 &: U_0(t) = \mathrm{L}^{-1}\left\{\tfrac{1}{s}\left(U(0) + \mathrm{L}\left\{u_0(t)\right\}\right)\right\} \\ p^1 &: U_1(x) = \mathrm{L}^{-1}\left\{-\tfrac{1}{s}\left(\mathrm{L}\left\{u_0(t) - A(t) - B(t)U_0(t) - C(t)U_0^2(t)\right\}\right)\right\} \\ p^j &: U_j(x) = \mathrm{L}^{-1}\left\{\tfrac{1}{s}\left(\mathrm{L}\left\{B(t)U_{j-1}(t) + C(t)\textstyle\sum_{k=0}^{j-1} U_k(t)U_{j-k-1}(t)\right\}\right)\right\}, \\ & \qquad\qquad\qquad\qquad\qquad\qquad\qquad\qquad\qquad\qquad j = 2,3,\ldots \end{aligned} \quad (10)$$

Suppose that the initial approximation has the form $U(0) = u_0(t) = \alpha$, therefore the exact solution may be obtained as following

$$u(t) = \lim_{p\to 1} U(t) = U_0(t) + U_1(t) + \cdots \tag{11}$$

3 Examples

xample 1. Consider the following quadratic Riccati differential equation taken from [1]

$$\begin{cases} u'(t) = 16t^2 - 5 + 8tu(t) + u^2(t), \\ u(0) = 1 \end{cases} \tag{12}$$

The exact solution of above equation was found to be of the form

$$u(t) = 1 - 4t. \tag{13}$$

To solve equation (12) by the LTNHPM, we construct the following homotopy

$$U'(t) - u_0(t) + p\left[u_0(t) + 5 - 16t^2 - 8tU(t) - U^2(t)\right] = 0 \tag{14}$$

Applying Laplace transform on both sides of (14), we have

$$\mathrm{L}\left\{U'(t) - u_0(t) + p\left[u_0(t) + 5 - 16t^2 - 8tU(t) - U^2(t)\right]\right\} = 0 \tag{15}$$

Using the differential property of Laplace transform we have

$$s\mathrm{L}\{U(t)\} - U(0) = \mathrm{L}\left\{u_0(t) - p\left[u_0(t) + 5 - 16t^2 - 8tU(t) - U^2(t)\right]\right\} \tag{16}$$

or

$$\mathrm{L}\{U(t)\} = \frac{1}{s}\left\{U(0) + \mathrm{L}\left\{u_0(t) - p\left[u_0(t) + 5 - 16t^2 - 8tU(t) - U^2(t)\right]\right\}\right\} \tag{17}$$

By applying inverse Laplace transform on both sides of (17), we have

$$U(t) = \mathrm{L}^{-1}\left\{\frac{1}{s}\left(U(0) + \mathrm{L}\left\{u_0(t) - p\left[u_0(t) + 5 - 16t^2 - 8tU(t) - U^2(t)\right]\right\}\right)\right\} \tag{18}$$

Suppose the solution of equation (18) to have the following form

$$U(t) = U_0(t) + pU_1(t) + p^2U_2(t) + \cdots, \tag{19}$$

where $U_i(t)$ are unknown functions which should be determined. Substituting equation (19) into equation (18), collecting the same powers of p and equating each coefficient of p to zero, results in

$$\begin{array}{l} p^0:\ U_0(t)=\mathrm{L}^{-1}\left\{\frac{1}{s}\left(U(0)+\mathrm{L}\left\{u_0(t)\right\}\right)\right\} \\ p^1:\ U_1(x)=\mathrm{L}^{-1}\left\{-\frac{1}{s}\left(\mathrm{L}\left\{u_0(t)+5-16t^2-8tU_0(t)-U_0^2(t)\right\}\right)\right\} \\ p^j:\ U_j(x)=\mathrm{L}^{-1}\left\{\frac{1}{s}\left(\mathrm{L}\left\{-8tU_{j-1}(t)+\sum_{k=0}^{j-1}U_k(t)U_{j-k-1}(t)\right\}\right)\right\} \\ \qquad\qquad\qquad\qquad\qquad\qquad\qquad\qquad\qquad\qquad\qquad\qquad\qquad\qquad j=2,3,\ldots \end{array} \tag{20}$$

Assuming $u_0(t)=U(0)=1$, and solving the above equation for $U_j(t)$, $j=0,1,\cdots$ leads to the result

$$\begin{array}{l} U_0(t)=1+t, \\ U_1(t)=\frac{5t}{3}\left(5t^2+3t-3\right), \\ U_2(t)=\frac{5t^2}{3}\left(10t^3+10t^2-8t-3\right), \\ U_3(t)=\frac{5t^3}{63}\left(425t^4+595t^3-399t^2-399t+63\right), \\ U_4(t)=\frac{t^4}{567}\left(38750t^5+69750t^4-36000t^3-72135t^2+7938t+8505\right), \\ \vdots \end{array}$$

Therefore we gain the solution of q. (12) as

$$u(t)=U_0(t)+U_1(t)+U_3(t)+\cdots=1-4t$$

which is exact solution.

xample 2. Consider the following quadratic Riccati differential equation taken from [13, 7, 14, 6, 8]

$$\begin{cases} u'(t)=1+2u(t)-u^2(t), \\ u(0)=0. \end{cases} \tag{21}$$

The exact solution of above equation was found to be of the form

$$u(t)=1+\sqrt{2}\tanh\left[\sqrt{2}t+\frac{1}{2}\log\left(\frac{\sqrt{2}-1}{\sqrt{2}+1}\right)\right] \tag{22}$$

The Taylor expansion of $u(t)$ about $t=0$ gives

$$u(t)=t+t^2+\frac{1}{3}t^3-\frac{1}{3}t^4-\frac{7}{15}t^5-\frac{7}{45}t^6+\frac{53}{315}t^7+\frac{71}{315}t^8+\cdots. \tag{23}$$

To solve equation (21), by the LTNHPM, we construct the following homotopy

$$U'(t)=u_0(t)-p\left[u_0(t)-1-2U(t)+U^2(t)\right] \tag{24}$$

Applying Laplace transform, we have

$$\mathrm{L}\left\{U'(t)-u_0(t)+pu_0(t)-p[1+2U(t)-U^2(t)]\right\}=0 \tag{25}$$

Using the differential property of Laplace transform we have

$$s\mathrm{L}\{U(t)\} - U(0) = \mathrm{L}\left\{u_0(t) - p\left[u_0(t) - 1 - 2U(t) + U^2(t)\right]\right\} \tag{26}$$

or

$$\mathrm{L}\{U(t)\} = \frac{1}{s}\left\{U(0) + \mathrm{L}\left\{u_0(t) - p\left[u_0(t) - 1 - 2U(t) + U^2(t)\right]\right\}\right\} \tag{27}$$

By applying inverse Laplace transform on both sides of (27), we have

$$U(t) = \mathrm{L}^{-1}\left\{\frac{1}{s}\left(U(0) + \mathrm{L}\left\{u_0(t) - p\left[u_0(t) - 1 - 2U(t) + U^2(t)\right]\right\}\right)\right\} \tag{28}$$

Suppose the solution of equation (28) to have the following form

$$U(t) = U_0(t) + pU_1(t) + p^2U_2(t) + \cdots, \tag{29}$$

where $U_i(t)$ are unknown functions which should be determined. Substituting equation (29) into equation (28), collecting the same powers of p , and equating each coefficient of p to zero, results in

$$\begin{array}{l} p^0:\ U_0(t) = \mathrm{L}^{-1}\left\{\frac{1}{s}\left(U(0) + \mathrm{L}\left\{u_0(t)\right\}\right)\right\} \\ p^1:\ U_1(x) = \mathrm{L}^{-1}\left\{-\frac{1}{s}\left(\mathrm{L}\left\{u_0(t) - 1 - 2U_0(t) + U_0^2(t)\right\}\right)\right\} \\ p^j:\ U_j(x) = \mathrm{L}^{-1}\left\{\frac{1}{s}\left(\mathrm{L}\left\{2U_{j-1}(t) + \sum_{k=0}^{j-1} U_k(t)U_{j-k-1}(t)\right\}\right)\right\},\ j = 2, 3, \ldots \end{array} \tag{30}$$

Assuming $u_0(t) = U(0) = 0$, and solving the above equation for $U_j(t)$, $j = 0, 1, \cdots$ leads to the result

$$\begin{array}{l} U_0(t) = 0, \\ U_1(t) = t, \\ U_2(t) = t^2, \\ U_3(t) = \frac{t^3}{3}, \\ U_4(t) = -\frac{t^4}{3}, \\ U_5(t) = -\frac{7t^5}{15}, \\ \vdots \end{array} \tag{31}$$

Therefore we gain the solution of equation (21) as

$$\begin{array}{l} u(t) = U_0(t) + U_1(t) + U_3(t) + \cdots \\ \quad = t + t^2 + \frac{1}{3}t^3 - \frac{1}{3}t^4 - \frac{7}{15}t^5 - \frac{7}{45}t^6 + \frac{53}{315}t^7 + \cdots, \end{array} \tag{32}$$

and this in the limit of infinitely many terms, yields the exact solution of (21).

xample 3. Consider the following quadratic Riccati differential equation taken from [1]

$$\begin{cases} u'(t) = \mathrm{e}^t - \mathrm{e}^{3t} + 2\mathrm{e}^{2t}u(t) - \mathrm{e}^t u^2(t), \\ u(0) = 1. \end{cases} \tag{33}$$

The exact solution of this equation is $u(t) = \mathrm{e}^t$. We construct the following homotopy

$$U'(t) - u_0(t) + p\left[u_0(t) - \mathrm{e}^{pt} + \mathrm{e}^{3pt} - 2\mathrm{e}^{2pt}U(t) + \sum_{n=0}^{\infty} \mathrm{e}^{pt}U^2(t)\right] = 0 \quad (34)$$

Applying Laplace transform on both sides of (34), we have

$$\mathrm{L}\left\{U'(t) - u_0(t) + p\left[u_0(t) - \mathrm{e}^{pt} + \mathrm{e}^{3pt} - 2\mathrm{e}^{2pt}U(t) + \sum_{n=0}^{\infty} \mathrm{e}^{pt}U^2(t)\right]\right\} = 0 \quad (35)$$

Using the differential property of Laplace transform we have

$$\begin{aligned} s\mathrm{L}\{U(t)\} - U(0) =& \mathrm{L}\Bigg\{u_0(t) - p\Big[u_0(t) - \mathrm{e}^{pt} \\ &+ \mathrm{e}^{3pt} - 2\mathrm{e}^{2pt}U(t) + \sum_{n=0}^{\infty} \mathrm{e}^{pt}U^2(t)\Big]\Bigg\} \end{aligned} \quad (36)$$

or

$$\begin{aligned} \mathrm{L}\{U(t)\} =& \frac{1}{s}\Bigg\{U(0) + \mathrm{L}\Big\{u_0(t) \\ &- p\Big[u_0(t) - \mathrm{e}^{pt} + \mathrm{e}^{3pt} - 2\mathrm{e}^{2pt}U(t) + \sum_{n=0}^{\infty} \mathrm{e}^{pt}U^2(t)\Big]\Big\}\Bigg\} \end{aligned} \quad (37)$$

By applying inverse Laplace transform on both sides of (37) and using the Taylor series of $e^{\alpha t} = \sum_{n=0}^{\infty} \frac{(\alpha t)^n}{n!}$, we have

$$\begin{aligned} U(t) =& \mathrm{L}^{-1}\Bigg\{\frac{1}{s}\Bigg(U(0) + \mathrm{L}\Big\{u_0(t) - p\Big[u_0(t) - \sum_{n=0}^{\infty} p^n \frac{t^n}{n!} \\ &+ \sum_{n=0}^{\infty} p^n \frac{(3t)^n}{n!} - 2\sum_{n=0}^{\infty} p^n \frac{(2t)^n}{n!}U(t) + \sum_{n=0}^{\infty} p^n \frac{t^n}{n!}U^2(t)\Big]\Big\}\Bigg)\Bigg\} \end{aligned} \quad (38)$$

Suppose the solution of U can be expanded into infinite series as $U(t) = \sum_{n=0}^{\infty} p^n U_n(t)$. Substituting $U(t)$ into equation (38), collecting the same powers of p , and equating each coefficient of p to zero, results in

$$\begin{aligned}
&p^0: \ U_0(t) = \mathrm{L}^{-1}\left\{\tfrac{1}{s}\left(U(0) + \mathrm{L}\left\{u_0(t)\right\}\right)\right\}\\
&p^1: \ U_1(x) = \mathrm{L}^{-1}\left\{-\tfrac{1}{s}\left(\mathrm{L}\left\{u_0(t) - 2U_0 + U_0^2\right\}\right)\right\}\\
&p^2: \ U_2(x) = \mathrm{L}^{-1}\left\{-\tfrac{1}{s}\left(\mathrm{L}\left\{2t - 4tU_0 - 2U_1 + tU_0^2 + 2U_0U_1\right\}\right)\right\}\\
&p^3: \ U_3(x) = \mathrm{L}^{-1}\{-\tfrac{1}{s}(\mathrm{L}\{4t^2 - 4tU_1 - 2U_2 - 4t^2U_0 + 2tU_0U_1\\
&\qquad\qquad +U_1^2 + 2U_0U_2 + \tfrac{1}{2}t^2U_0^2\})\}\\
&\vdots
\end{aligned} \tag{39}$$

Assuming $u_0(t) = U(0) = 1$, and solving the above equation for $U_j(t)$, $j = 0, 1, \cdots$ leads to the result

$$\begin{aligned}
&U_0(t) = 1 + t,\\
&U_1(t) = -\tfrac{t^3}{3},\\
&U_2(t) = -\tfrac{t^2}{12}\left(-6 - 8t + t^2\right),\\
&U_3(t) = -\tfrac{t^3}{5040}\left(840 - 4620t + 504t^2 - 840t^3 - 240t^4 + 35t^5\right)\\
&\vdots
\end{aligned} \tag{40}$$

Therefore we gain the solution of equation (33) as

$$\begin{aligned}
u(t) &= U_0(t) + U_1(t) + U_3(t) + \cdots\\
&= 1 + t + \tfrac{1}{2!}t^2 + \tfrac{1}{3!}t^3 + \cdots\\
&= \textstyle\sum_{n=0}^{\infty} \frac{t^n}{n!} = e^t,
\end{aligned} \tag{41}$$

which is exact solution.

xample 4. Consider the following quadratic Riccati differential equation taken from [13, 7, 14, 6, 8]

$$\begin{cases} u'(t) = -u(t) + u^2(t),\\ u(0) = \frac{1}{2} \end{cases} \tag{42}$$

The exact solution of above equation was found to be of the form

$$u(t) = \frac{\mathrm{e}^{-t}}{1 + \mathrm{e}^{-t}} \tag{43}$$

The Taylor expansion of $u(t)$ about $t = 0$ gives

$$u(t) = \frac{1}{2} - \frac{1}{4}t + \frac{1}{48}t^3 - \frac{1}{480}t^5 + \frac{17}{80640}t^7 - \frac{31}{1451520}t^9 + \frac{691}{319334400}t^{11} - \cdots. \tag{44}$$

To solve equation (43) by the LTNHPM, we construct the following homotopy:

$$U'(t) = u_0(t) - p\left[u_0(t) + U(t) - U^2(t)\right] \tag{45}$$

By applying Laplace transform we get

$$\mathrm{L}\{U(t)\} = \frac{1}{s}\left\{U(0) + \mathrm{L}\left\{u_0(t) - p\left[u_0(t) + U(t) - U^2(t)\right]\right\}\right\} \tag{46}$$

Using inverse Laplace transform on both sides of (46), we have

$$U(t) = \mathrm{L}^{-1}\left\{\frac{1}{s}\left(U(0) + \mathrm{L}\left\{u_0(t) - p\left[u_0(t) + U(t) - U^2(t)\right]\right\}\right)\right\} \tag{47}$$

Suppose the solution of equation (47) to have the following form

$$U(t) = U_0(t) + pU_1(t) + p^2U_2(t) + \cdots, \tag{48}$$

Substituting equation (48) into equation (47), collecting the same powers of p , and equating each coefficient of p to zero, results in

$$\begin{array}{l} p^0:\ U_0(t) = \mathrm{L}^{-1}\left\{\frac{1}{s}\left(U(0) + \mathrm{L}\left\{u_0(t)\right\}\right)\right\} \\ p^1:\ U_1(x) = \mathrm{L}^{-1}\left\{-\frac{1}{s}\left(\mathrm{L}\left\{u_0(t) + U_0(t) - U_0^2(t)\right\}\right)\right\} \\ p^j:\ U_j(x) = \mathrm{L}^{-1}\left\{\frac{1}{s}\left(\mathrm{L}\left\{-U_{j-1}(t) + \sum_{k=0}^{j-1} U_k(t)U_{j-k-1}(t)\right\}\right)\right\},\ j = 2, 3, \ldots \end{array} \tag{49}$$

Assuming $u_0(t) = U(0) = \frac{1}{2}$, and solving the above equation for $U_j(t)$, $j = 0, 1, \cdots$ leads to the result

$$\begin{array}{l} U_0(t) = \frac{1}{2}(1+t), \\ U_1(t) = \frac{t}{12}\left(-9 + t^2\right), \\ U_2(t) = \frac{t^3}{60}\left(-15 + t^2\right), \\ U_3(t) = \frac{t^3}{5040}\left(945 - 387t^2 + 17t^4\right), \\ U_4(t) = \frac{t^5}{45360}\left(5103 - 918t^2 + 31t^4\right), \\ U_5(t) = \frac{t^5}{4989600}\left(-280605 + 227205t^2 - 25575t^4 + 691t^6\right), \\ \vdots \end{array} \tag{50}$$

Therefore we gain the solution of equation (42) as

$$\begin{aligned} u(t) &= U_0(t) + U_1(t) + U_3(t) + \cdots \\ &= \tfrac{1}{2} - \tfrac{1}{4}t + \tfrac{1}{48}t^3 - \tfrac{1}{480}t^5 + \tfrac{17}{80640}t^7 - \tfrac{31}{1451520}t^9 + \tfrac{691}{319334400}t^{11} - \cdots, \end{aligned} \tag{51}$$

this in the limit of infinitely many terms, yields the exact solution of (42).

4 Conclusion

In the present work, we proposed a combination of Laplace transform method and homotopy perturbation method to solve nonlinear Riccati differential equation. The new method developed in the current paper was tested on several examples. The obtained results show that these approaches can solve the problem effectively. Unlike the previous approach implemented by the

present authors, so-called NHPM, the present technique, does not need the initial approximation to be defined as a power series. In the NHPM we reach to a set of recurrent differential equations which must be solved consecutively to give the approximate solution of the problem. Sometimes we have to do many computations in order to reach to the higher orders of approximation with acceptable accuracy. Also as an advantage of the LTNHPM over decomposition procedure of Adomian, the former method provides the solution of the problem without calculating Adomian's polynomials. The advantage of the LTNHPM over numerical methods (finite difference, finite element, ...) and ADM is that it solves the problem without any need to discretization of the variables. The Computations finally lead to a set of nonlinear equations with one unspecified value in each equation. The results show that the LTNHPM is an effective mathematical tool which can play a very important role in nonlinear sciences.

References

1. Abbasbandy, S. *A new application of He's variational iteration method for quadratic Riccati differential equation by using Adomian's polynomials,* J. Comput. Appl. Math., 207 (2007), 59–63.

2. Abbasbandy, S. *Homotopy perturbation method for quadratic Riccati differential equation and comparison with Adomian's decomposition method*, Appl. Math. Comput., 174 (2006), 485–490.

3. Abbasbandy, S. *Iterated He's homotopy perturbation method for quadratic Riccati differential equation*, Appl. Math. Comput., 175 (2006), 581–589.

4. Aminikhah, H. and Biazar, J. *A new HPM for ordinary differential equations*, Numerical Methods for Partial Differential quations, 26 (2009), 480–489.

5. Aminikhah, H. and Biazar, J. *A new HPM for ordinary differential equations*, Numer. Methods Partial Differ. quat., 26 (2009), 480–489.

6. Aminikhah, H. and Hemmatnezhad, M. *An efficient method for quadratic Riccati differential equation,* Commun. Nonlinear Sci. Numer. Simul., 15 (2010) 835–839.

7. Biazar, J. and Aminikhah, H. *Study of convergence of homotopy perturbation method for systems of partial differential*, Computers & Mathematics with Applications, 58 (2009), 2221–2230.

8. Biazar, J. and Ghazvini, H. *Exact solutions for nonlinear Schrodinger equations by He's homotopy perturbation method*, Physics Letters A, 366 (2007), 79–84.

9. Carinena, J. F., Marmo, G., Perelomov, A. M. and Ranada, M. F. *Related operators and exact solutions of Schrodinger equations,* Int. J. Mod. Phys. A, 13 (1998), 4913–4929.

10. l-Tawil, M. A., Bahnasawi, A. A. and Abdel-Naby, A. *Solving Riccati differential equation using Adomian's decomposition method,* Appl. Math. Comput., 157 (2004),503–514.

11. Ganji, D. D. *The application of He's homotopy perturbation method to nonlinear equations arising in heat transfer*, Physics Letters A, 355 (2006), 337–341.

12. Ganji, D. D. and Sadighi, A. *Application of homotopy perturbation and variational iteration methods to nonlinear heat transfer and porous media equations*, Journal of Computational and Applied Mathematics, 207 (2007), 24–34.

13. Geng, F., Lin, Y. and Cui, M. *A piecewise variational iteration method for Riccati differential equations,* Comput. Math. Appl., 58 (2009), 2518–2522.

14. He, J. H. *Homotopy perturbation technique*, Computer Methods in Applied Mechanics and ngineering, 178 (1999), 257–262.

15. Liao, S. *Comparison between the homotopy analysis method and homotopy perturbation method*, Applied Mathematics and Computation, 169 (2005), 1186–1194.

16. Reid, W. T. *Riccati Differential Equations*, Academic Press, New York, 1972.

17. Scott, M. R. *Invariant Imbedding and its Applications to Ordinary Differential Equations*, Addison-Wesley, 1973.

18. Tan, Y. and Abbasbandy, S. *Homotopy analysis method for quadratic Riccati differential equation,* Commun. Non-linear Sci. Numer. Simulation, 13 (2008), 539–546.

Iranian J. of Numerical Anal sis and Optimization
Vol 3, No. 2, 2013 , pp 33-46

Homotopy perturbation and Elzaki transform for solving Sine-Gorden and Klein-Gorden equations

. Hesameddini and N. Abdollahy

Abstract

In this paper, the homotop perturbation method H M and Elzaki transform is emplo ed to obtain the approximate anal tical solution of the Sine Gorden and the Klein Gorden e uations. The nonlinear terms can be handled b the use of homotop perturbation method. The proposed homotop perturbation method is applied to reformulate the first and the second order initial value problems hich leads to the solution in terms of transformed variable, and the series solution that can be obtained b making use of the inverse transformation.

ey ords: Homotopy-perturbation method; lzaki transform; Sine-Gorden equation; lein-Gorden equation.

1 Introduction

In this paper, we have considered the Sine-Gorden (SG) and lein-Gorden (G) equations, as the following and also in [2] respectively:

$$u_{tt} - u_{xx} + \alpha g(u) = f(x,t), \tag{1}$$

and

$$u_{tt} - u_{xx} + \beta_1 u + \beta_2 g(u) = f(x,t), \tag{2}$$

where u is a function of x, t and g is a nonlinear function . The α parameter is so-called dissipative term, which is assumed to be a real number with $\alpha \geq 0$. When $\alpha = 0$, q. (1), reduces to the undamped SG equation, and when $\alpha > 0$, to the damped one. f is also a known analytic function. The Sine-Gorden and lein-Gorden equations model many problems in classical and Quantum mechanics, solitons, and condensed matter physics

Recieved 2 Februar 2013; accepted 12 June 2013
E. Hesameddini
Department of Mathematics, Facult of Basic Sciences, Shiraz niversit of Technolog .O.Box 71555-313, Shiraz, Iran. e-mail hesameddini sutech.ac.ir

N. Abdollah
Department of Mathematics, Facult of Basic Sciences, Shiraz niversit of Technolog .O.Box 71555-313, Shiraz, Iran. e-mail n.abdollah sutech.ac.ir

[1, 5]. The SG equation arose in a strict mathematical context in differential geometry in the theory of surfaces of constant curvature [17]. For the SG equation, the exact soliton solution have been obtained in [16], using Hirotas method in [21], using Lambs method in [18], by Bäcklund transformation and painlevé transcendents in [18]. Numerical solutions for the undamped SG equation have been given among others by Guo et al. [8] by use of two diffirent schemes, Xin [24] who studied SG equation as an asymptotic reduction of the two-level dissipationless Max well-Bloch system, Christiansen and Lomdahl [3] used a generalized leapforg method and Argyris et al. found the accurate and efficient methods for solving such equations which is an active research undertaken by Herbst et al. The method [14], presented a numerical solution for the SG equation obtained by means of an explicit symplectic behavior of a double-discrete, completely integrable discretization of the Sine-Gorden equation, and they have illustrated their technique by numerical experiments. Wazwaz [23] has used the tanh method to obtain the exact solution of SG equation. Approximate analytical solution of line Gorden equation thrangh the Adomian Decomposition Method (ADM) was presented in [4, 6, 20]. aya has applied the modified ADM (MADM) for obtaining the approximate analytical solution of the Sine-Gorden equation in [19]. Another more powerful and convenient analytical technique, called the homotopy-perturbation method (HPM), was first developed by He [13]. Some part of this work on HPM can be found in [9, 10, 11]. HPM transformes a difficult problem into a set of problems which are easier to solve. Chowdhury and Hashim [2], have used the HPM to obtain the approximate analytical solution of Sine-Gorden and lein-Gorden equations. Recently, Tarig lzaki [7], has introduced a new integral transform, named the lzaki transform, and it has further applied to the solution of ordinary and partial differential equations.

Now, we consider in this work the effectiveness of the homotopy-perturbation lzaki transform method to obtain the exact and approximate analytical solution of the Sine-Gorden and the lein-Gorden equations.

2 Elzaki Transform

The basic definition of modified form of Sumudo transform or lzaki transform is defiend as follow, lzaki transform of the function $f(t)$ is:

$$E[f(t)] = \upsilon \int_0^\infty f(t)e^{-t/\upsilon}dt, \qquad t > 0. \tag{3}$$

Tarig M. lzaki showed the modified form of Sumudu transform or lzaki transform in which it is applied to the differential equations, ordinary dif-

ferential equations, system of ordinary, partial differential equations, and integral equations.

To obtain the lzaki transform of partial derivative, we use the integration by part, and then we have:

$$E[\frac{\partial f(x,t)}{\partial t}] = \frac{1}{\upsilon}T(x,\upsilon) - \upsilon f(x,0), \tag{4}$$

$$E[\frac{\partial^2 f(x,t)}{\partial t^2}] = \frac{1}{\upsilon^2}T(x,\upsilon) - f(x,0) - \upsilon\frac{\partial f(x,t)}{\partial t}, \tag{5}$$

$$E[\frac{\partial f(x,t)}{\partial x}] = \frac{d}{dx}T(x,\upsilon), \tag{6}$$

$$E[\frac{\partial^2 f(x,t)}{\partial x^2}] = \frac{d^2}{dx^2}T(x,\upsilon). \tag{7}$$

Proof: First, we assume

$$\upsilon\int_0^\infty \frac{\partial f}{\partial t}e^{\frac{-t}{\upsilon}}dt = T(x,\upsilon). \tag{8}$$

By using the integration by parts one obtain:

$$\begin{aligned} E[\frac{\partial f(x,t)}{\partial t}] &= \int_0^\infty \upsilon\frac{\partial f}{\partial t}e^{\frac{-t}{\upsilon}}dt = \lim_{p\to\infty}\int_0^\infty \upsilon e^{\frac{-t}{\upsilon}}\frac{\partial f}{\partial t}dt \\ &= \lim_{p\to\infty}\{[\upsilon e^{\frac{-t}{\upsilon}}f(x,t)]_0^p - \int_0^p e^{\frac{-t}{\upsilon}}f(x,t)dt\} \\ &= \frac{T(x,\upsilon)}{\upsilon} - \upsilon f(x,0). \end{aligned} \tag{9}$$

Assuming that f is a piecewise continuous function and $\frac{\partial f}{\partial x}$ exist, also it is of exponential order which is means that there exist nonegative constants M and T such that for all $t \geq T$, we have

$$|f(t)| \leq Me^{at}.$$

Now,

$$E[\frac{\partial f(x,t)}{\partial x}] = \int_0^\infty \upsilon\frac{\partial f(x,t)}{\partial x}e^{\frac{-t}{\upsilon}}dt, \tag{10}$$

using the Leibnitz rule to find:

$$E[\frac{\partial f(x,t)}{\partial x}] = \frac{d}{dx}T(x,\upsilon). \tag{11}$$

By using this method, we have:

$$E[\frac{\partial^2 f(x,t)}{\partial x^2}] = \frac{d^2}{dx^2}T(x,\upsilon). \tag{12}$$

To find:

$$E[\frac{\partial^2 f(x,t)}{\partial t^2}]. \tag{13}$$

Let:

$$\frac{\partial f(x,t)}{\partial t} = g, \tag{14}$$

then we have:

$$E[\frac{\partial^2 f(x,t)}{\partial t^2}] = E[\frac{\partial g(x,t)}{\partial t}] = E\frac{[g(x,t)]}{\upsilon} - \upsilon g(x,0), \tag{15}$$

$$E[\frac{\partial^2 f(x,t)}{\partial t^2}] = \frac{1}{\upsilon^2}T(x,\upsilon) - f(x,0) - \upsilon\frac{\partial f(x,t)}{\partial t}. \tag{16}$$

Therefore, one can easily extend this result to the *nth* partial derivative by using mathematical induction. We will see that, the lzaki transform rivals the Laplace transform in solving the problem, its main advantage is the rivals that it may be used to solve problems without resorting to a new frequency domain because it preserve scales and units properties, the lzaki transform may be used to solve intricate problems in engineering, mathematics and applied science without resorting to a new frequency domain.

3 Homotopy Perturbation Method:

The basic idea of the standard HPM was given by He [9, 12] and a new interpretation of this technique was presented by our research gorup [15]. To introduce HPM, considered the following general nonlinear differential equation:

$$Lu + Nu = f(x,t), \tag{17}$$

with initial conditions:

$$u(x,0) = k_1, \quad u_t(x,0) = k_2. \tag{18}$$

Where u is a function of x, t and k_1, k_2 are constants or functions of x. Also L and N are the linear and nonlinear operators respectively. According to HPM [2] we construct a homotopy which satisfies the following relation:

$$H(u,p) = Lu - L\nu_0 + p[L\nu_0 + Nu - f(x,t)] = 0, \tag{19}$$

where $p \in [0,1]$ is an embedded parameter and ν_0 is an arbitrary initial approximation satisfing the given initial condition.
By setting $p = 0$ and $p = 1$ in q. (19), one obtain:

$$H(u,0) = Lu - L\nu_0 = 0, \qquad \text{and} \qquad H(u,1) = Lu + Nu - f(x,t) = 0, \tag{20}$$

which are the linear and nonlinear original equations, respectively. In topology, this is called deformation and $Lu - L\nu_0$ and $Lu + Nu - f(x,t)$ are called homotopic. Here, the embedded parameter is introduced much more naturally, unaffected by artificial factor, further it can be considered as a small parameter for $0 \leq p \leq 1$.

Chowdhury and Hashim in [2], have presented an alternative way for choosing the initial approximation, that is:

$$\nu_0 = u(x,0) + tu_t(x,0) + L^{-1}f(x,t) = k_1 + tk_2 + L^{-1}f(x,t), \tag{21}$$

where $L^{-1}(.) = \int_0^t \int_0^t ... \int_0^t (.)dt...dtdt$ depends on the order of the linear operator. With this assumption that the initial approximation ν_0 given in q. (21), in HPM, the solution of q. (19), is expressed as:

$$u(x,t) = u_0(x,t) + pu_1(x,t) + p^2u_2(x,t) + ... \tag{22}$$

Hence the approximate solution of q. (17), can be expressed as a power series of p, i. e.

$$u = \lim_{p \to 1} u = \sum_{i=0}^{\infty} u_i. \tag{23}$$

4 Homotopy Perturbation and Elzaki Transform Method:

Consider a general nonlinear partial differential equation with initial conditions of the form:

$$Du(x,t) + Ru(x,t) + Nu(x,t) = f(x,t), \tag{24}$$

$$u(x,0) = c_1, \qquad u_t(x,0) = c_2. \tag{25}$$

Where D is a linear differential operator of order two, R is a linear differential operator of less order than D , N is the general nonlinear differential operator, $f(x,t)$ is the source term and c_1, c_2 are constants or functions of x.

By taking lzaki transform to both sides of q.(24), result in:

$$E[Du(x,t)] + E[Ru(x,t)] + E[Nu(x,t)] = E[f(x,t)]. \tag{26}$$

Using the differentiation property of lzaki transform and the initial condition in q.(24), one obtain:

$$E[u(x,t)] = v^2E[f(x,t)] + v^2c_1 + v^3c_2 - v^2E[R(x,t) + Nu(x,t)]. \tag{27}$$

Applying the inverse lzaki transform on both sides of q.(27), we get:

$$u(x,t) = F(x,t) - E^{-1}\{\upsilon^2 E[Ru(x,t) + Nu(x,t)]\}, \tag{28}$$

where $F(x,t)$ represent the term arising from the source term and the prescribed initial conditions.

According to HPM we have:

$$u(x,t) = F(x,t) - pE^{-1}\{\upsilon^2 E[Ru(x,t) + Nu(x,t)]\}, \tag{29}$$

now by substituting

$$u(x,t) = \sum_{i=0}^{\infty} p^i u_i(x,t), \qquad N[u(x,t)] = \sum_{i=0}^{\infty} p^i H_i(u), \tag{30}$$

in q. (29) where $H_i(u)$ is He's polynomials that are given by:

$$H_i(u_0, u_1, ..., u_i) = \frac{1}{i!}\frac{\partial}{\partial p^i}[N(\sum_{i=0}^{\infty} p^i u_i)]_{p=0}, \qquad i = 0, 1, 2, ..., \tag{31}$$

one obtain:

$$\begin{aligned}\sum_{i=0}^{\infty} p^i u_i(x,t) =& F(x,t) \\ & - p\{E^{-1}[\upsilon^2 E[(R\sum_{i=0}^{\infty} p^i u_i(x,t)) + N(\sum_{i=0}^{\infty} p^i H_i(u))]]\}.\end{aligned} \tag{32}$$

This our method is infact a coupling technique of lzaki transform and the homotopy perturbation method. Comparing the coefficients of the like powers of p the following approximations are resulted:

$$\begin{aligned} p^0 &: u_0(x,t) = F(x,t), \\ p^1 &: u_1(x,t) = -E^{-1}\{\upsilon^2 E[Ru_0(x,t) + H_0(u)]\}, \\ p^2 &: u_2(x,t) = -E^{-1}\{\upsilon^2 E[Ru_1(x,t) + H_1(u)]\}, \\ &\vdots \\ & etc. \end{aligned}$$

Therefore the solution will be obtained as:

$$u(x,t) = u_0(x,t) + u_1(x,t) + u_2(x,t) + ... \tag{33}$$

5 Numerical Applications

In this section, we apply the homotopy-perturbation and lzaki transform method for solving Sine-Gorden and lein-Gorden equations. Numerical results are very encouraging.

xample .1 First, consider the following Sine-Gorden equation with the given initial conditions:

$$u_{tt} - u_{xx} + \sin u = 0, \quad u(x,0) = 0, \quad u_t(x,0) = 4\mathrm{sech(x)}. \tag{34}$$

The exact solution is given in [2] as:

$$u(x,t) = 4\arctan[t\mathrm{sech(x)}]. \tag{35}$$

To solve the example by this method, we take $\sin u \simeq u - \frac{u^3}{6} + \frac{u^5}{120}$.

After taking lzaki transform of (34), subjected to the initial conditions, one obtain:

$$E[(u(x,t)] = 4\upsilon^3\mathrm{sech(x)} + \upsilon^2\frac{\mathrm{d}^2}{\mathrm{dx}^2}\ [(\mathrm{u(x,t)}] - \upsilon^2\ [\mathrm{u} - \frac{\mathrm{u}^3}{6} + \frac{\mathrm{u}^5}{120}]. \tag{36}$$

The inverse lzaki transform implies that:

$$u(x,t) = 4t\mathrm{sech(x)} + \ ^{-1}\{\upsilon^2\frac{\mathrm{d}^2}{\mathrm{dx}^2}\ [(\mathrm{u(x,t)}] - \upsilon^2\ [\mathrm{u} - \frac{\mathrm{u}^3}{6} + \frac{\mathrm{u}^5}{120}]\}. \tag{37}$$

Now applying the homotopy perturbation method, we get:

$$\begin{aligned}\sum_{i=0}^{\infty} p^i u_i(x,t) = 4t\mathrm{sech(x)} + \mathrm{p}\{\upsilon^2\frac{\mathrm{d}^2}{\mathrm{dx}^2}\ [\sum_{\mathrm{i=0}}^{\infty}\mathrm{p^i u_i(x,t)}] \\ - \upsilon^2 E[\sum_{i=0}^{\infty} p^i u_i(x,t) - \frac{(\sum_{i=0}^{\infty} p^i u_i(x,t))^3}{6} + \frac{(\sum_{i=0}^{\infty} p^i u_i(x,t))^5}{120}]\}.\end{aligned} \tag{38}$$

By comparing the coefficients of the same powers of p, result in:

$$\begin{aligned} p^0 &: u_0(x,t) = 4t\mathrm{sech(x)}, \\ p^1 &: u_1(x,t) = \frac{d^2}{dx^2}E^{-1}\{4t\mathrm{sech(x)}\upsilon^2\ \ (\mathrm{t})\} - \ ^{-1}\{4\mathrm{tsech(x)}\upsilon^2\ \ (\mathrm{t})\} \\ &\quad + E^{-1}\{\frac{64}{6}\mathrm{sech^3(x)}\upsilon^2\ \ (\mathrm{t}^3)\} - \ ^{-1}\{\frac{1024}{120}\mathrm{sech^5(x)}\upsilon^2\ \ (\mathrm{t}^5)\}. \end{aligned}$$

Then, we get:

$$p^1 : u_1(x,t) = \frac{4}{315}\mathrm{sech}^5(\mathrm{x}) - (-105\mathrm{t}^3\cosh^2(\mathrm{x}) + 42\mathrm{t}^5\cosh^2(\mathrm{x}) - 16\mathrm{t}^7),$$

$$\begin{aligned} p^2 : u_2(x,t) = \frac{4}{2027025}t^5\mathrm{sech}^9(\mathrm{x})(7040\mathrm{t}^8 - 33696\mathrm{t}^9\cosh^2(\mathrm{x}) - 4290\mathrm{t}^4\cosh^4(\mathrm{x}) \\ + 143000t^4\cosh^2(x) - 205920t^2\cosh^4(x) + 51480t^2\cosh^6(x) \\ - 270270\cosh^6(x) + 405405\cosh^4(x), \end{aligned}$$

therefore, the 3-terms lzaki-HPM solution is:

$$\begin{aligned} u(x,t) = \frac{4}{2027025}t\mathrm{sech}^9(\mathrm{x})(7040\mathrm{t}^{12} - 33696\mathrm{t}^{10}\cosh^2(\mathrm{x}) - 4290\mathrm{t}^8\cosh^4(\mathrm{x}) \\ + 143000t^8\cosh^2(x) - 308880t^6\cosh^4(x) + 51480t^6\cosh^6(x) \\ + 405405t^4\cosh^4(x) - 675675t^2\cosh^6(x) - 270270\cosh^8(x). \end{aligned}$$

The behavior of the solution (34), by 4-terms of HPM and its exact solution are shown in Figures 1 and 2.

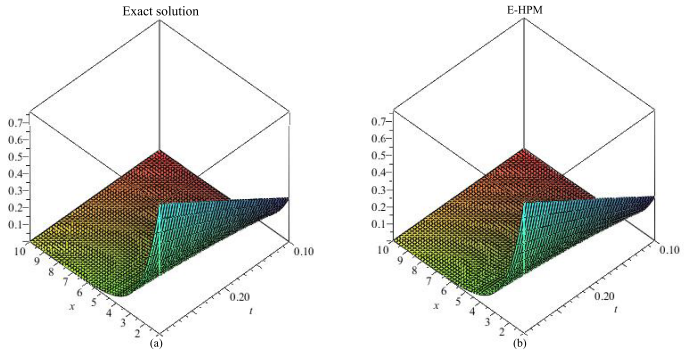

Figure 1: These surfaces show the approximate solutions obtained by 4-terms of HPM and the exact solution of $u(x,t)$, respectively .(a) xact plot; (b) HPM plot(q. (35))

xample .2 Considering the following Sine-Gorden equation with the given initial conditions:

$$u_{tt} - u_{xx} + \sin u = 0, \qquad u(x,0) = \pi + \varepsilon\cos(\mu x), \quad u_t(x,0) = 0. \quad (39)$$

Where $\mu = \frac{\sqrt{2}}{2}$ and ε is a constant.

We take $\sin u \simeq u - \frac{u^3}{6} + \frac{u^5}{120}$ to solve this example.

By taking lzaki transform of (39), subjected to the initial conditions,we have:

$$E[u(x,t)] = \upsilon^2(\pi + \varepsilon\cos(\mu x)) + \upsilon^2\frac{d^2}{dx^2}E[u(x,t)] - \upsilon^2 E[u - \frac{u^3}{6} + \frac{u^5}{120}](40)$$

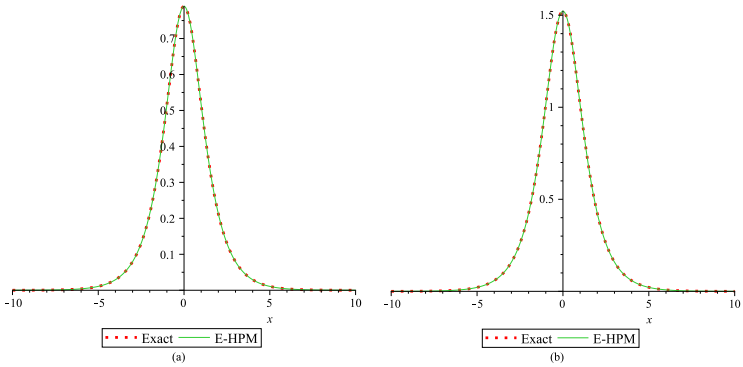

Figure 2: Comparison of the results by HPM with the exact solution for example 5.1.

Table 1: Comparison of the exact and numerical solutions of example 5.1

x	t	xact solution	HPM-4term	Absolute error
0	0	0	0	0
0.062	0.162	0.6412071928	0.6412071885	4.3×10^{-9}
0.156	0.156	0.6116706532	0.6116706503	2.9×10^{-9}
0.469	0.469	1.5964486815	1.596478333	$.8482 \times 10^{-7}$
0.539	0.403	1.349539812	1.349538454	$.1358 \times 10^{-6}$
0.620	0.685	2.077035544	2.076989415	$.0590 \times 10^{-9}$
0.781	0.781	2.136014353	2.135871203	$.1431 \times 10^{-7}$
0.896	0.893	2.234155992	2.233473035	$.6829 \times 10^{-7}$
0.975	0.992	2.319920856	2.317982103	$.1938 \times 10^{-7}$
1.000	1.000	2.300024730	2.297874130	$.2150 \times 10^{-7}$

The inverse lzaki transform implies that:

$$u(x,t) = (\pi + \varepsilon\cos(\mu x))E^{-1}[\upsilon^2] + E^{-1}\{\upsilon^2\frac{d^2}{dx^2}E[(u(x,t)] - \upsilon^2 E[u] + \upsilon^2 E[\frac{u^3}{6}] - \upsilon^2\frac{[u^5]}{120}\}.$$

Now applying the homotopy perturbation method, result in:

$$u(x,t) = (\pi + \varepsilon\cos(\mu x))E^{-1}[\upsilon^2] + p\{E^{-1}\{\upsilon^2\frac{d^2}{dx^2}E[(u(x,t)] - \upsilon^2 E[u] + \upsilon^2 E[\frac{u^3}{6}] - \upsilon^2\frac{[u^5]}{120}\}\}.$$

By taking $u(x,t) = \sum_{i=0}^{\infty} p^i u_i(x,t)$ and comparing the coefficients of the same powers of p, one obtain:

$$\begin{aligned}
p^0 &: u_0(x,t) = (\pi + \varepsilon\cos(\mu x)),\\
p^1 &: u_1(x,t) = \frac{t^2}{2}\{-\mu^2\varepsilon\cos(\mu x) + \frac{1}{6}(\pi+\varepsilon\cos(\mu x))^3 - \frac{1}{120}(\pi+\varepsilon\cos(\mu x))^5\\
&\quad - (\pi+\varepsilon\cos(\mu x))\}.\\
&\vdots\\
&etc.
\end{aligned}$$

Therefore, the 3-terms lzaki-HPM solution is:

$$\begin{aligned}
u(x,t) &= \pi + \varepsilon\cos(\mu x) + \frac{t^2}{2}\{-\mu^2\varepsilon\cos(\mu x) + \frac{1}{6}(\pi+\varepsilon\cos(\mu x))^3 - \frac{1}{120}\\
&\quad (\ \pi+\varepsilon\cos(\mu x))^5 - (\pi+\varepsilon\cos(\mu x))\} + \frac{1}{69120}[\varepsilon^2\cos^2(\mu x) + 9\pi\varepsilon^8\cos^8(\mu x)\\
&\quad + (36\pi^2-32)\varepsilon^7\cos^7(\mu x) + (84\pi^3-224\pi)\varepsilon^6\cos^6(\mu x)\\
&\quad + 720(\mu^2 + \frac{7}{40}\pi^4 - \frac{14}{15}\pi^2 + \frac{8}{15})\varepsilon^5\cos^5(\mu x)\\
&\quad + 2400\pi(\frac{21}{400}\pi^4 + \frac{4}{5} + \mu^2 - \frac{7}{15}\pi^2)\varepsilon^4\cos^4(\mu)(x)\\
&\quad - 480(\varepsilon^2\mu^2 + (-6\pi^2+12)\mu^2 - 8\pi^2 + \frac{7}{3}\pi^4 - \frac{7}{40}\pi^6 + \varepsilon)\varepsilon^3\cos^3(\mu x)\\
&\quad - 1440\pi(\varepsilon^2\mu^2 + (-\pi^2+6)\mu^2 + \frac{7}{15}\pi^4 - \frac{1}{40}\pi^6 - \frac{8}{3}\pi^2 + \varepsilon)\varepsilon^2\cos^2(\mu x)\\
&\quad - 1440(\mu^2\varepsilon^2(\pi^2-2) - 2\mu^4 + \{\frac{-1}{6}\pi^4 - 4 + 2\pi^2\}\mu^{24} + \frac{7}{45}\pi^6\\
&\quad + 4\pi^2 - \frac{1}{160}\pi^8) - \frac{4}{3}\pi^4 - 2)\varepsilon\cos(\mu x) - 480\pi(\pi^2-6)\mu^2\varepsilon^2\\
&\quad + 384\pi^5 + 2880\pi - 1920\pi^3 + \pi^9 - 32\pi^7]t^4.
\end{aligned}$$

The behavior of the solution (39), by 4-terms of HPM and its HPM solution are shown in Figure 3.

xample .3 Considering the following lein-Gorden equation with the given initial conditions:

$$u_{tt} - u_{xx} = u, \qquad u(x,0) = 1 + \sin x, \qquad u_t(x,0) = 0. \tag{41}$$

Taking lzaki transform of (41), subjected to the initial condition, one obtain:

$$E[(u(x,t)] = (1+\sin x)\upsilon^2 + \upsilon^2 E[u] + \upsilon^2\frac{d^2}{dx^2}E[u]. \tag{42}$$

The inverse lzaki transform implies that:

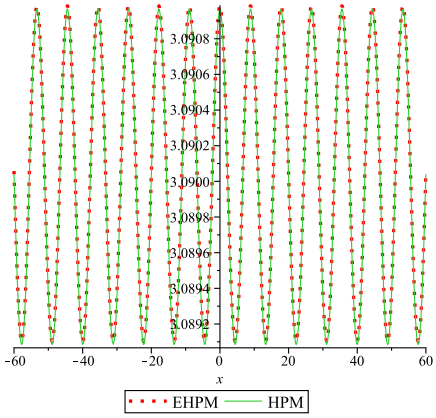

Figure 3: Comparison of the results by HPM with the HPM solution for example 5.2.

$$u(x,t) = 1 + \sin x + E^{-1}\{\upsilon^2 E[u] + \upsilon^2 \frac{d^2}{dx^2} E[u]\}. \tag{43}$$

Now, applying the homotopy perturbation method, we get:

$$u(x,t) = 1 + \sin x + p\{E^{-1}\{\upsilon^2 E[u] + \upsilon^2 \frac{d^2}{dx^2} E[u]\}\}. \tag{44}$$

By taking $u(x,t) = \sum_{i=0}^{\infty} p^i u_i(x,t)$ and comparing the coefficients of the same powers of p, result in:

$$\begin{aligned} p^0 &: u_0(x,t) = 1 + \sin x, \\ p^1 &: u_1(x,t) = \frac{t^2}{2}, \\ p^2 &: u_2(x,t) = \frac{t^4}{24}, \\ p^3 &: u_3(x,t) = \frac{t^6}{720}, \\ &\vdots \\ &etc. \end{aligned}$$

Therefore, the 4-terms approximate series solution is:

$$u(x,t) = 1 + \sin x + \frac{t^2}{2} + \frac{t^4}{24} + \frac{t^6}{720}, \tag{45}$$

and this will, in the limit of infinitely many terms, yield the closed form solution [6],

$$u(x,t) = \sin x + \cosh t. \tag{46}$$

xample .4 Consider the following lein-Gorden equation with the given initial conditions:

$$u_{tt} - u_{xx} = -u, \qquad u(x,0) = 0, \qquad u_t(x,0) = x. \tag{47}$$

Taking lzaki transform of (47), subjected to the initial conditions, one obtain:

$$E[(u(x,t)] = x\upsilon^3 + \upsilon^2 \frac{d^2}{dx^2} E[u] - \upsilon^2 E[u]. \tag{48}$$

The inverse lzaki transform implies that:

$$u(x,t) = tx + E^{-1}\{\upsilon^2 \frac{d^2}{dx^2} E[u] - \upsilon^2 E[u]\}. \tag{49}$$

Now applying the homotopy perturbation method, we get:

$$u(x,t) = tx + p\{E^{-1}\{\upsilon^2 \frac{d^2}{dx^2} E[u] - \upsilon^2 E[u]\}\}. \tag{50}$$

By taking $u(x,t) = \sum_{i=0}^{\infty} p^i u_i(x,t)$ and comparing the coefficients of the same powers of p, one obtain:

$$\begin{aligned}
p^0 &: u_0(x,t) = tx, \\
p^1 &: u_1(x,t) = \frac{-xt^3}{3!}, \\
p^2 &: u_2(x,t) = \frac{+xt^5}{5!}, \\
p^3 &: u_3(x,t) = \frac{-xt^7}{7!}, \\
&\vdots \\
&etc.
\end{aligned}$$

Thus, the 4-terms approximate series solution is:

$$u(x,t) = tx - \frac{xt^3}{3!} + \frac{xt^5}{5!} - \frac{xt^7}{7!}, \tag{51}$$

and this will, in the limit of infinitely many terms, yield the closed form solution [22],

$$u(x,t) = x \sin t. \tag{52}$$

6 Conclusion:

In this paper, the lzaki Homotopy-Perturbation method (HPM) has been successfully employed to obtain the approximate analytical solutions of the Sine-Gorden and the lein-Gorden equations. In example 5.3, the obtained result by this method is almost accurate and very near to the exact solution, also in example 5.4, it is observed that the (HPM) solution yields the exact solution in only few iterations. Therefore, this novel iterative method has a bright aspect in future to obtain the approximate analytical solutions of ordinary and partial differential equations.

References

1. Caudrey P., libeck I. and Gibbon J. *The sine-gorden equation as a model classical field theory*, Nuovo cimento, 25 (1975), 496–511.
2. Chowdhury, M. S. H. and Hashim, I. *Application of homotopy-perturbation method to Kline-Gorden and Sine-Gorden equations*, Chaos, Solitons Fractals, 39 (2009), 1928-1935.
3. Christiansen P. L. and Lomdahl, P. S. *Numerical solution of 2+1 dimensional Sine-Gordon solitons*, Phys 2D (1981), 482-494.
4. Deeba, . and huri, S. *A decomposition method for solving the nonlinear Kline-gorden equation*, J Comput Phys, 124 (1996), 442-448.
5. Dodd P., libeck I. and Gibbon J. *salitons and nonlinear wave equation*, London Academic, 1982.
6. l-Sayad S. *The decomposition method for studying the Kline-Gordon equation*, Chaos, Soliton Fractals, 18 (2003), 1025–1030.
7. lzaki T. M. and Hilal, . M. A. *Homotopy perturbation and Elzaki transform for solving nonlinear partial differential equations*, Mathematical Theory and Modling, 2 (2012), 3, 33-42.
8. Guo, B. Y., Pascual, P. J., Rodriguez, M. J. and Vzquez, L. *Numerical solution of the Sine-Gorden equation,* Appl Math comput, 18 (1986), 1–14.
9. He J. *A copuling method of homotopy technique and perturbation technique for nonlinear problem*, Int J Nonlinear Mech, 35 (2000), 37-43.

10. He J. *Homotopy-perturbation method for solving boundary value problem*, Phys Lett A, 350 (2006), 87-88.

11. He J. *Non-perturbative methods for strongly nonlinear problems*, Germanay: Die Deutsche bibliothek, 2006.

12. He J. *Some asymptotic method for strongly nonlinear equations*, Int J Mod Phys B, 20 (2006), 1141-1199.

13. He J. *Varuational iteration method-a kind of non-linear analytical technique: some examples*, Int J Nonlinear mech, 34 (1999), 699–708.

14. Herbst B. and Ablowitz M. *Numerical homoclinic instabilities in the Sine-Gorden equation*, Quaest Math, 15 (1992), 345–630.

15. Hesameddini, . and Latifizadeh, H. *A new vision to the He's homotopy perturbation method*, Nonlinear sci. simul., 10 (2009), 1389–1398.

16. Hirota, R. *Exact three-soliton solution of the two-dimensional Sine-Gorden equation*, J Phys Soc Jpn, 35 (1973), 15–66.

17. Hu H. C. and Lou, S. Y. *New guasi-periodic waves of the (2+1)dimensional Sine-Gorden system*, Phys Lett A, 341 (2005), 422–426.

18. aliappan, P. and Lakshmanan, M *Kadomstev-Petviashvili two-dimensional Sine-Gorden equations: reduction to painleve transcendents*, J Phys A, 12 (1979), 249–252.

19. aya D. *A numerical solution of the Sine-Gorden equation using the modified decomposition method*, Appl Math Comput, 143 (2003, 309–317.

20. aya D. and l-Sayed S. *A numerical solution of the Kline-Gordon equation and convergence of the decomposition method*, Appl Math Comput, 156 (2004), 341–353.

21. Leibbrandt, G. *New exact solutions of the classical Sine-Gorden equation in 2+1 and 3+1 dimensionals*, Phys Rev Lett, 41 (1978), 435–438.

22. Mohyud-Din, S. T. and Yildirim A. *Variatonal Iteration Method for solving Kline-Gordon equation*, JAMSI, 6 (2010), 1, 99–106.

23. Wazwaz A. *The tanh method: exact solution of Sine-Gordon and the sinh-Gordon equations*, Appl Math Comput, 167 (2005), 1196–1210.

24. Xin, J. X. *Modeling light bullets with the two-dimensional Sine-Gordon equation*, Phys D, 135 (2000), 345–368.

Iranian J. of Numerical Anal sis and Optimization
Vol 3, No. 2, 2013 , pp 47-65

A shape-measure method for solving free-boundary elliptic systems with boundary control function

A. Fakharzadeh Jahromi

Abstract

This article deals ith a computational algorithmic approach for obtaining the optimal solution of a general free boundar problem governed b an elliptic e uation ith boundar control and functional criterion. After determining the eak solution of the s stem, the problem is converted into a variational format. Then, b using some aspects of measure theor , the method characterize the nearl optimal pair of domain and its related optimal control function at the same time. This method has man advantages such as strong linearit , automatic existence theorem and the abilit of obtaining global solution. T o sets of numerical examples is also given.

ey ords: lliptic controlled system; Weak solution; Atomic measure; Linear programming; Free boundary problem.

1 Introduction and background

The class of elliptic partial differential equations includes many important systems encountered in mechanics and geometry. Indeed an industrial setting time is spent setting up the allowable set of shapes (domains of equations) in order to get a feasible solution. The structural optimization of such systems has more commonly been applied in the automobile, marine and aerospace industries designing and even in a simple mechano-chemical model of a biomolecular processes (see [9], [1] and [2]). A large part of these problems deals with the free boundary problems when a part of domain's boundary is fixed and the rest is varied. The understanding of models of equations and free boundary problems (such as Monge-Amper equation) may have significant geometric even topological applications. For instance, for an inhomogeneous free boundary problem, Vogel obtained the convexity or starlikeness of variable part when the fixed part is convex or starlike [23]. Furthermore, Lancaster showed that the method of curves of constant direction could be used to investigate even the quasilinear and fully nonlinear

Recieved 23 Februar 2013; accepted 12 June 2013
A. Fakharzadeh Jahromi
Department of Mathematics, Shiraz niversit of Technolog , .O.Box 7155-313, Shiraz, Iran. e-mail a_fakharzadeh sutech.ac.ir

elliptic free boundary problems [12]. Munch recently have done some works based on topological and numerical approaches (see for instance [14] and [15]). The main goal in structural optimization is to computerize the design process and therefore shorten the time it takes to create a new design or to improve an existing one. Therefore, the results on mechanical formulation of the problems, their functional analysis and on control theory have recently been combined. For a review of such results the reader is referenced to [9] and [10]. Indeed, the optimal control theory provides the basic techniques for computing the derivatives of criteria functions with respect to the boundary. Thus in essence, the optimal control and optimization may be applied when the control becomes associated with the shape of domain. In the former, most of the induced solution methods from control theory, were focused on applications of the principles of the calculus of variations (such as Hadamard works [8]). However in the latter, studies were made only for those problems with an explicit solution for PD 's. ventually the methods were extended to problems of structural engineering; in particular, those were possible to be converted into an optimal control problem with control governed by the coefficients of PD 's [18]. In this manner the numerical methods (Finite lement, Finite Difference, Boundary lement,...) and Computer Aided Design technology within the optimization loop are used for fully computerizing the design loop. However, the problems are encountered with numerical discretization [18]. In 1986, Rubio in [19], introduced the embedding method for solving the optimal control problems governed by ordinary differential equations, by use of positive Radon measures; then it was employed to obtain the optimal control for a system governed by partial differential equations; like [11] for diffusion and [20] for elliptic systems. The method was based on the strong properties of measures and has many advantages.
Since 1999 till know, by helping of this method, we have solved different cases of the optimal shape design problems governed by elliptic systems (a brief report of this is given in [5]). After solving the problem in polar coordinates in [3], the based measure theoretical approached was improved to cartezian coordinates but for solving optimal shape problem in [4]. Then, we improved the method for optimal shape design problems with distributed control function in [5] To continue, in the present paper we introduce an approach for solving free boundary problems governed by elliptic equations with two special characteristics. Herein, the system is involved with a boundary control function as appears in industrial applications. Moreover, the geometry of domains is completely in the general case.

2 Problem in classical form

As a geometrical point of view, we consider $D \subset R^2$ as a bounded region with a piecewise-smooth, closed and simple boundary ∂D which consists of

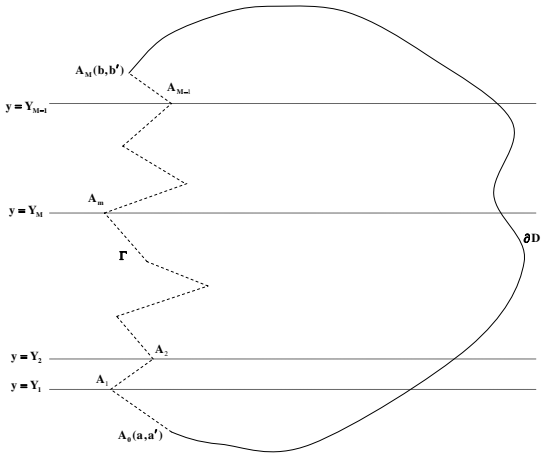

Figure 1: A general domain$D$ and its boundary ∂D.

a fixed and a variable part (cure), denoted by Γ. It is joining two known points $A = (a, a')$ and $B = (b, b')$ so that $a' \leq b'$ and it makes ∂D simple and closed (see Figure 1). By applying the idea of approximating a curve with broken lines, Γ can be approximated by a finite number of connected segments; we fix this number as $M + 1$. Therefore, each Γ can be considered as an $M + 1$ connected segments in which the initial and the final points of them belong to Γ (see Figure 1). If these points are denoted by $A_0 = A, A_1, \ldots, A_{M+1} = B$, then any appropriate region D (domain) can be represented by points $A_m = (x_m, y_m), m = 1, 2, \ldots, M$.
Indeed the variable part of ∂D (and hence D) is represented with $2M$ variables $x_1, x_2, \ldots, x_M$ and $y_1, y_2, \ldots, y_M$. We fix the y-component of each point A_m as $y_m = Y_m \in R$ for $m = 1, 2, \ldots, M$, so that $a' < Y_1 < Y_2 < \cdots < Y_M < b'$.[0] This would not decries the generalities; since even y_m is fixed, but x_m is varied and hence A_m could be any place on the half line $y(x) = Y_m$ with the vertex on the fixed part of D. Therefore the segments $A_m A_{m+1}, m = 0, 1, \ldots, M$, could be selected so that the set of them approximates Γ well enough.
Let $f \in C(D \times R)$ and $g \in C(D)$, be two given real valued functions. The above domain D is called *admissible* if the elliptic equation

$$\Delta u(X) + f(X, u) = g(X)\ ,\ u_{|_{\partial D}} = v, \tag{1}$$

has a bounded solution on the domain D; here it is also supposed that $X = (x, y) \in D$, $u : D \to R$ is a bounded trajectory function which takes values in

[0] For special case like $a' = b'$, one can fix the x-components of points A_m's instead of y-components.

the bounded set U, and $v : \partial D \to R$ is a bounded boundary control function, which is Lebesgue measurable and taks values in a bounded set V.

As mentioned, the variable part of ∂D can be approximated with M number of unknown corners. For a fixed positive integer M, the set of all admissible domains is denoted by $\mathcal{D}_M$. When $M \longrightarrow \infty$, if an appropriate optimal shape design problem in $\mathcal{D}_M$ has a minimizer, then this may tend in some topology to the minimizer over $\mathcal{D}$ (the set of all general admissible domains) if such exists. However things can go wrong; for instance: There may be no minimizer over $\mathcal{D}_M$; there may be no minimizer over $\mathcal{D}$; or both $\mathcal{D}$ and $\mathcal{D}_M$; the sequence of minimizer over $\mathcal{D}_M$ may not be convergent or may tend in some sense towards a curve that does not define a shape. Young in [24] has shown that their related subsequence of broken lines, tends to an infinitesimal zigzag (generalized curve). This is not (necessarily) an admissible curve. So the solution over $\mathcal{D}_M$ does not tend to the solution over $\mathcal{D}$, even in the weakly*-sense. Also, there is the important point that too oscillatory boundaries (like the infinitesimal zigzag) sometimes cause problem; Pironneau in [18] shows some of these problems. Hence, we prefer to fix the number M in this paper, and search for the optimal solution of the appropriate problems over $\mathcal{D}_M$.

For a given admissible domain $D \in \mathcal{D}_M$, let $f_1 : D \times U \longrightarrow R$ and , $f_2 : \partial D \times V \longrightarrow R$ be two continuous, non- negative, real-valued functions; further, we assume that there is a constant $L > 0$ so that $\mid f_1(X, u(X)) \mid \leq L \mid u \mid$. We define the functional performance criteria, as

$$\mathbf{I}(D, v) = \int_D f_1(X, u(X))\, dX + \int_{\partial D} f_2(s, v(s))\, ds, \tag{2}$$

where u is the bounded solution of (1). We also define $\mathbf{F}$ as the set of all pairs of (D, v) where $D \in \mathcal{D}_M$ and v is the boundary control function. With the above assumption, we are going to solve the following optimal shape design problem on $\mathbf{F}$:

$$\begin{aligned} &\textbf{Minimize}: && \mathbf{I}(D, v) = \int_D f_1(X, u(X))\, dX + \int_{\partial D} f_2(s, v(s))\, ds \\ &\textbf{Subject to}: && \Delta u(X) + f(X, u) = g(X)\ ,\ u_{|_{\partial D}} = v, \end{aligned} \tag{3}$$

(For some industrial applications of this problem, the reader can have a look on [18]).

To identify the optimal domain in $\mathcal{D}_M$, D^*, and its associated optimal control function, $v^*_{D^*}$, we apply the method which we call shape-measure [5]. This approach characterizes the optimal pair of domain and its related optimal control function in two stages; first for a given domain $D \in \mathcal{D}_M$, by applying the embedding method and use of the Radon measures power, the related optimal control problem will be solved. Then in the next stage, a standard minimization algorithm will be applied to determine the nearly

optimal pair of domain and its related optimal control function at the same time.

3 Problem in new formulation

In general, even for a fixed domain, it is difficult to characterize a classical bounded solution for the elliptic equation (1). Therefore, one can change the problem into the other form in which a bounded *weak* (generalized) solution of (1) is involved.

Proposition 1. : *Let u be the classical solution of (1), then we have the following integral equality:*

$$\int_D (u\Delta\psi + \psi f)\, dX - \int_{\partial D} v(\bigtriangledown\psi.\mathbf{n})\, ds = \int_D \psi g\, dX,\ \forall\psi \in H_0^1(D). \qquad (4)$$

that here $\mathbf{n}$ *is the outward unit vector on* ∂D.

Proof. By multiplying (1) with the function $\psi \in H_0^1(D)$ (the set of functions in the Sobolev space of order 1 in which they are zero on ∂D), integrating over D, and then using the Green's formula (see [13]), one can obtain the equality (4). □

Now, by regarding [5], let D be a fixed domain; then the mentioned optimal free boundary problem changes into an optimal control one in which the same functional as $\mathbf{I}$ must be minimized over the set of all admissible pairs of trajectory and control functions on D. We define $\Omega = D\times U$ and $\omega = \partial D\times V$; then, a bounded weak solution and its corresponded control function define a pair of positive and linear functional $u(\cdot) : F \longrightarrow \int_D F(X, u(X))dX$ and $v(\cdot) : G \longrightarrow \int_{\partial D} G(s, V(s))ds$ on $C(\Omega)$ and $C(\omega)$ respectively. As shown in [19] and [20], the Riesz Representation Theorem [21] shows that there are measures μ_u and ν_v so that:

$$\mu_u(F) = u(F),\ \forall F \in C(\Omega)\ ;\ \nu_v(G) = v(G),\ \forall F \in C(\omega).$$

So far, we have just changed the appearance of the problem. Indeed the transformation between the pair of trajectory and controls, (u, v), and the pair of measures (μ_u, ν_v), is injection (see [19]). Now we extend the underlying space and consider the minimization of the problem over the set of all pairs of measures (μ, ν) in $\mathcal{M}^+(\Omega)\times\mathcal{M}^+(\omega)$ satisfying the mentioned conditions plus the extra properties $\mu(\xi) = \int_D \xi(X)\, dX = a_\xi$ and $\nu(\tau) = \int_{\partial D} \tau(s)\, ds = b_\tau$; these are deduced from the definition of an admissible pair (u, v) and they indicate that the measures μ and ν project on the (x, y)-plan and real line respectively, as Lebesgue measures. We remind the reader that here it is supposed $\xi : \Omega \longrightarrow R$ in $C(\Omega)$ depends only on variable $X = (x, y)$ (i.e. $\xi \in C_1(\Omega)$), and $\tau : \omega \longrightarrow R$ in $C(\omega)$ depends only on variable s (i.e. $\tau \in C_1(\omega)$).

Therefore, we are going to solve the following problem:

$$\begin{aligned} \textbf{Minimize}: \quad & \mathbf{i}(\mu,\nu) := \mu(f_1) + \nu(f_2) \\ \textbf{Subject to}: \quad & \mu(F_\psi) + \nu(G_\psi) = c_\psi, \ \forall \psi \in H_0^1(D); \\ & \mu(\xi) = a_\xi, \qquad\qquad \forall \xi \in C_1(\Omega); \\ & \nu(\tau) = b_\tau, \qquad\qquad \forall \tau \in C_1(\omega), \end{aligned} \tag{5}$$

where $F_\psi = u\Delta\psi + \psi f$, $G_\psi = -v(\bigtriangledown\psi.\mathbf{n} \mid_{\partial D})$ and $c_\psi = \int_D \psi g \, dX$. This new formulation has some advantages; for instance, it is linear in respect to the unknown measure, and if we denote $Q \subset \mathcal{M}^+(\Omega) \times \mathcal{M}^+(\omega)$ as the set of all pairs of measures (μ, ν) satisfying the conditions mentioned in (5), then Q is compact in the sense of the weak* topology (see for instance [5]). Moreover the function $(\mu, \nu) \in Q \longrightarrow \mu(f_1) + \nu(f_2) \in R$ is continuous. Thus by Proposition $II.1$ of [19], the problem (5) definitely has a minimizer in Q. The theoretical measure problem (5) is an infinite-dimensional linear program problem; even there is no any identified method for obtaining the solution directly, but its solution can be achieved by choosing the countable sets of functions that are uniformly dense (total), in the appropriate spaces. Let $\{\psi_i : i = 1, 2, 3, \dots\}$, $\{\xi_j : j = 1, 2, 3, \dots\}$, and $\{\tau_l : l = 1, 2, 3, \dots\}$, be total sets in the spaces $H_0^1(D)$, $C_1(\Omega)$ and $C_1(\omega)$ respectively. By choosing just a finite number of these functions, the problem (5) is changed into the following one:

$$\begin{aligned} \textbf{Minimize}: \quad & \mathbf{i}(\mu,\nu) = \mu(f_1) + \nu(f_2) \\ \textbf{Subject to}: \quad & \mu(F_i) + \nu(G_i) = c_i, \qquad i = 1, 2, \dots, M_1; \\ & \mu(\xi_j) = a_j, \qquad\qquad j = 1, 2, \dots, M_2; \\ & \nu(\tau_l) = b_l, \qquad\qquad l = 1, 2, \dots, M_3, \end{aligned} \tag{6}$$

where $F_i := F_{\psi_i}, G_i := G_{\psi_i}, c_i := c_{\psi_i}$, $a_j := a_{\xi_j}$ and $b_l := b_{\tau_l}$. As proved in [5] Theorem 2, the solution of (6) tends to the solution of (5) whenever $M_1, M_2, M_3 \longrightarrow \infty$; hence the solution of (5) can be approximated by one from (6) when the positive integers M_1, M_2 and M_3 are chosen large enough. Now one can construct a suboptimal pair of trajectory and control functions for the functional $\mathbf{i}$ via the optimal solution, (μ^*, ν^*), of (6).

4 Atomic measures and discretization

The problem (6) is a semi-infinite linear programming problem; the number of equations is finite but the underlying space is not a finite-dimensional space. Despite of some possibility for solving such problems (for instance see [7]), it is much more convenient if we could estimate its solution by a finite LP. The pair of optimal measures of (6) can be characterized by a result

of Rosenbloom's work which is shown in [19]; by introducing appropriate dense subsets in Ω and ω, one can conclude that μ^* and ν^* have the form $\mu^* = \sum_{n=1}^{N} \alpha_n \delta(Z_n)$ and $\nu^* = \sum_{k=1}^{K} \beta_k \delta(z_k)$ where $Z_n, n = 1, 2, \ldots, N$, and $z_k, k = 1, 2, \ldots, K$, belong to dense subsets of Ω and ω respectively and $\delta(t)$ is the unitary atomic measure with support the singleton set $\{t\}$. Hence, by defining a discretization on Ω and ω with the nodes $Z_n = (x_n, y_n, u_n)$, $n = 1, 2, \ldots, N$, and $z_k, k = 1, 2, \ldots, K$, the solution of (6) can be obtained by solving the following problem in which its unknowns are the coefficients $\alpha_n, n = 1, 2, \ldots, N$, and $\beta_k, k = 1, 2, \ldots, K$.

$$
\begin{aligned}
\textbf{Minimize}: & \sum_{n=1}^{N} \alpha_n f_1(Z_n) + \sum_{k=1}^{K} \beta_k f_2(z_k) \\
\textbf{Subject to}: & \sum_{n=1}^{N} \alpha_n F_i(Z_n) + \sum_{k=1}^{K} \beta_k G_i(z_k) = c_i,\ i = 1, 2, \ldots, M_1; \\
& \sum_{n=1}^{N} \alpha_n \xi_j(Z_n) = a_j, \qquad j = 1, 2, \ldots, M_2; \\
& \sum_{k=1}^{K} \beta_k \tau_l(z_k) = b_l, \qquad l = 1, 2, \ldots, M_3; \\
& \alpha_n \geq 0, \qquad n = 1, 2, \ldots, N; \\
& \beta_k \geq 0, \qquad k = 1, 2, \ldots, K;.
\end{aligned}
\tag{7}
$$

The result of this problem introduces a pair of measures (μ^*, ν^*) that the value of $\mathbf{i}(\mu^*, \nu^*)$, will be minimum; this pair serves the suboptimal pair of trajectory and control functions $(u_{v_D^*}, v_D^*)$. Thus for the fixed domain D, the minimum value of the functional $\mathbf{I}$ in the problem (3) is approximated as $\mathbf{I}(D, v_D^*) \equiv \mathbf{i}(\mu^*, \nu^*)$.

5 Searching the optimal curve (domain)

For a given domain, we have explained that how one can find the optimal control v_D^* for the problem (3), so that the value of $\mathbf{I}(D, v_D^*)$ is minimum. To obtain the minimum value of the performance criterion $\mathbf{I}(D, v)$ on $\mathbf{F}$, for each domain $D \in \mathcal{D}_M$, as explained, the variable part of its boundary is defined by a set of points like $\{A_m = (x_m, Y_m), m = 1, 2, \ldots, M\}$. Thus, for a given $D \in \mathcal{D}_M$, by solving the appropriate finite linear programming problem in (7), the nearly optimal value for $\mathbf{I}(D, v)$ (i.e. $\mathbf{I}(D, v_D^*) \equiv \mathbf{i}(\mu^*, \nu^*)$) is calculated as a function of the variables $x_1, x_2, \ldots, x_M$. Consequently, one can define the following function, which is a vector function of variables $x_1, x_2, \ldots, x_M$:

$$
\mathbf{J} \ : \ D \in \mathcal{D}_M \ \longrightarrow \ \mathbf{I}(D, v_D^*) \in R. \tag{8}
$$

Now to find the optimal pair of domain (or variable curve) and its related control function in $\mathbf{F}$, say $(D^*, v^*_{D^*})$, which solves the problem (3), it is enough to find the minimizer of $\mathbf{J}$.
The global minimizer of the vector function $\mathbf{J}$, say $(x_1^*, x_2^*, \ldots, x_M^*)$, can be identified by using one of the appropriate standard minimization search methods, like method introduced by Nelder and Mead in [16]; these algorithms usually need an initial set of components (initial domain) to start the process of minimization (we suppose that they give the global minimizer). ach time that the algorithm wants to calculate a value for $\mathbf{J}$, a finite LP problem like (7) should be solved. Whenever it reaches to the minimum value for $\mathbf{J}$, the minimizer $(x_1^*, x_2^*, \ldots, x_M^*)$ (the optimal curve) and therefore its associated optimal control function have been obtained. So, the optimal domain and its corresponding optimal control are determined at the same time; this is one of the main advantage of this method. Similar to the Proposition 5 of [5], one can easily prove that the method is convergence.

6 Numerical tests

For the following numerical works, we choose a countable total sets of functions in each spaces $H_0^1(D)$, $C_1(\Omega)$ and $C_1(\omega)$, that is, so that the linear combinations of these functions are uniformly dense (dense in the topology of uniform convergence) in the appropriate spaces. We know that the vector space of polynomials with the variable x and y, $P(x, y)$, is dense in $C^\infty(\overline{D})$; therefore the set

$$P_0(x, y) = \{p(x, y) \in P(x, y) \mid p(x, y) = 0, \forall (x, y) \in \partial D\},$$

is dense (uniformly) in $\left\{h \in C^\infty(\overline{D}) : h_{|_{\partial D}} = 0\right\} \equiv C_0^\infty(\overline{D})$. Since the set

$$Q(x, y) = \left\{1, x, y, x^2, xy, y^2, x^3, x^2y, xy^2, y^3, \ldots\right\}$$

is a countable base for the vector space $P(x, y)$, each elements of $P(x, y)$ and also $P_0(x, y)$, is a linear combination of the elements in $Q(x, y)$. By Theorem 3 of [13] page 131, the space $C^\infty(\overline{D})$ is dense in $H^1(D)$; thus the space $C_0^\infty(\overline{D})$ will be dense in $H_0^1(D)$. Consequently, the space $P_0(x, y)$ is uniformly dense in $H_0^1(D)$. Therefore, we define the function ψ_i for each i as

$$\psi_i(x, y) = q_D(x, y)q_i(x, y), \tag{9}$$

where q_i is an element of the countable set $Q(x, y)$ and $q_D(x, y)$ is a polynomial depended on D so that it is zero on ∂D (it will be defined separately for each example). Therefore $\psi_{i_{|_{\partial D}}} = 0$ and the set $\{\psi_i(x, y) : i = 1, 2, \ldots\}$ is total (uniformly dense in the topology of the uniform convergence) in $H_0^1(D)$.
Note: We remind the reader that Rubio and others (like Farahi and amyad

[6] and [11]) avoids to use the polynomials for such purposes; they usually prefer to apply the related functions defined by *sin* and *cos* or combinations of them. To be sure that these polynomials are suitable to determine the shape, we applied them first for determination the inside and the boundary of a circle (as an example of a shape) by applying the embedding method. For this purpose we used the Stock's theorem for these functions to show the relationship between the inside region and the boundary. The results was very good so that the most obtained inner points (28 from 30) was inside the circle and the rest (two other points) were close enough to the boundary.

For the second set (and also similarly the third one) of functions in (7), let L be a given positive integer number and divide D into L (not necessary equal) parts $D_1, D_2, \ldots, D_L$, so that by increasing L the area of each $D_s, s = 1, 2, \ldots, L$, will be decreased. Then, for each $s = 1, 2, \ldots, L$, we define:

$$\xi_s(x, y, u) = \begin{cases} 1 & (x, y) \in D_s \\ 0 & \text{otherwise} \end{cases}$$

These functions are not continuous, but each of them is the limit of an increasing sequence of positive continuous functions,$\{\xi_{s_k}\}$; then if μ is any positive Radon measure on Ω, $\mu(\xi_s) = \lim_{k\to\infty} \mu(\xi_{s_k})$. Now consider the set $\{\xi_j : j = 1, 2, \ldots, L\}$ of all such functions, for all positive integer L. The linear combination of these functions can approximate a function in $C_1(\Omega)$ arbitrary well (see [19] chapter 5).
By defining $U = V = [-1.0, 1.0]$ and $g(X) = 0$, in the following, two examples for the linear and nonlinear cases of the elliptic equations will be presented.

xample 6.1 Let the fixed part of the boundary of D consists of three sides of a unit square joining points $A = (1, 0), (0, 0), (0, 1)$ and $B = (1, 1)$; and a variable unknown curve joining points A and B, so that it makes ∂D simple and closed. Therefore $q_D(x, y)$ in (9) can be chosen as $xy(y-1)\prod_{l=1}^{M}(x - x_l + y - Y_l)$; in this manner, $\psi_i(x, y)$ is selected so that it is zero on each unknown corner $A_m = (x_m, Y_m)$ of Γ. Reminding that we are able to choose it in a way that it would be zero on each segment $A_{m-1}A_m$ (something which is done in the next example). Now we take $f_2(s, v) = 0$,

$$f_1(X, u) = \begin{cases} 400 & \text{-0.05} \le u \le 0.05 \\ \frac{1}{u^2} & \text{otherwise,} \end{cases}$$

and also $M = 8$, $Y_1 = 0.15$, $Y_2 = 0.25$, $Y_3 = 0.35$, $Y_4 = 0.45$, $Y_5 = 0.55$, $Y_6 = 0.65$, $Y_7 = 0.75$, $Y_8 = 0.85$. The control function is supposed to be zero on ∂D except the segment of line $y = 1$ which along this segment, $v(s)$ takes values in V, when $s \in [0, 1]$. Thus, in (7) we have $G_i = -(\frac{\partial \psi_i(s,y)}{\partial y})_{|_{y=1}}$.
To set up the finite linear programming (7) for the next two cases, we choose $M_1 = 3$ and $M_2 = M_3 = 10$. Also the condition $0 \le x_m \le 2, m = 1, 2, \ldots, 8$, is applied by using the penalty method (see [22]). Moreover we put a dis-

cretization on Ω with $N = 1100$ nodes by points $Z_n = (x_n, y_n, u_n)$, $n = 1, 2, \ldots, N$. Because the control function is zero on ∂D except the segment of the line $y = 1$, we have put a discretization on ω with $K = 110$ nodes like $z_k = (s_k, v_k), k = 1, 2, \ldots, K$; these nodes have been chosen as $z_k = z_{11(i-1)+j}$ for $i = 1, 2, \ldots, 10$ and $j = 1, 2, \ldots, 11$, where $s_{11(i-1)+j} = \frac{(i-1)+0.5}{10}$ and $v_{11(i-1)+j} = \frac{2(j-1)}{10} - 1.0$. Hence the total number of variables in a similar problem to (7) is $1100 + 110 = 1210$. In the case of these concepts, we solved the following examples for the linear and nonlinear case of the elliptic equations; in each case we chose the subroutine $AMOEBA$ (see [17]) as the standard minimization algorithm with the initial valves $X_m = 1.0$, for $m = 1, 2, \ldots, 8$ (indeed, here the initial domain is selected as a unit square). Also, we applied the $E04MBF$ NAG-Library Routine for solving the appropriate finite linear program.

inear Case: In this example for the linear case, we chose $f = 0$; then by applying the mentioned method, after 497 iteration we achieved the optimal value of $\mathbf{I} = 0.44432256772971$. The value of the variables in the final step was

$$X_1 = 0.044671, X_2 = 0.000003, X_3 = 0.000018, X_4 = 0.083868, X_5 = 0.004590,$$

$$X_6 = 1.181268, X_7 = 0.003360, X_8 = 1.291424.$$

According to the obtained results, the suboptimal control function, the initial and the final domain, and also the changes diagram of the objective function according to the number of iterations, have been plotted in the Figures 2, 3 and 4. We remind that one could do some smoothness and get better results (see xample 6.2 for instance).

Nonlinear case: By choosing $f = 5u^2$ and applying the other assumption as above, the example for the nonlinear case of the elliptic equations was solved. After 492 iterations, the optimal value was $\mathbf{I} = 0.44432182922939$ and the value of the variables in the final step was $X_1 = 0.044691, X_2 = 0.083889, X_3 = 0.004568, X_4 = 0.003356, X_5 = 0.000026, X_6 = 0.000001, X_7 = 1.181291, X_8 = 1.291379$. The results have introduced the suboptimal control function, the final domain and the changes diagram of the objective function which have been plotted in the Figures 5, 6 and 7.

xample 6.2 Let the fixed part of the boundary be the left half of the unite circle, joining the points $A = (0, -1)$ and $B = (0, 1)$. Hence for $M = 9$, $q_D(x, y)$ in (9) can be chosen as

$$(x+\sqrt{1-y^2})(x-5X_1(y+1))(x-5X_9(y-Y_9))\prod_{l=2}^{9}(x-X_{l-1}-5(X_l-X_{l-1})(y-Y_{l-1})),$$

where $Y_1 = -0.8$, $Y_2 = -0.6$, $Y_3 = -0.4$, $Y_4 = -0.2$, $Y_5 = 0$, $Y_6 = 0.2$, $Y_7 = 0.4$, $Y_8 = 0.6$, $Y_9 = 0.8$. This function is zero on all ∂D and thus in (7)

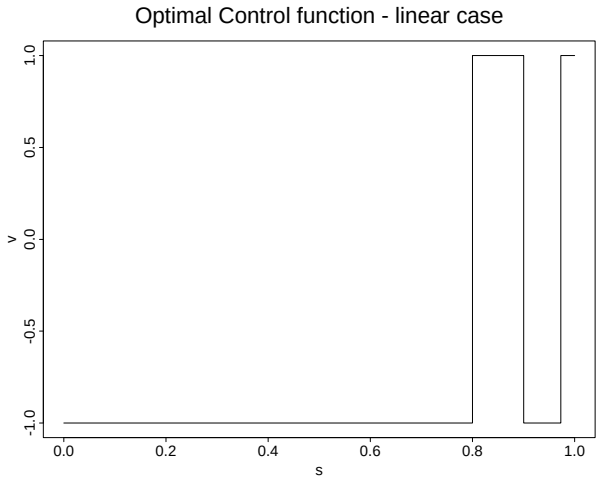

Figure 2: The optimal boundary control function for the linear case of x-ample 6.1.

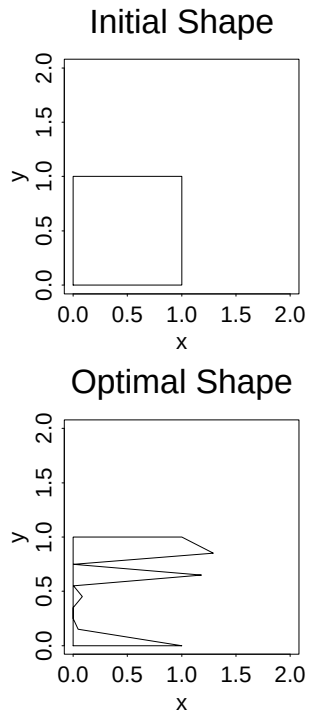

Figure 3: The initial and the optimal domain for the linear case of xample 6.1.

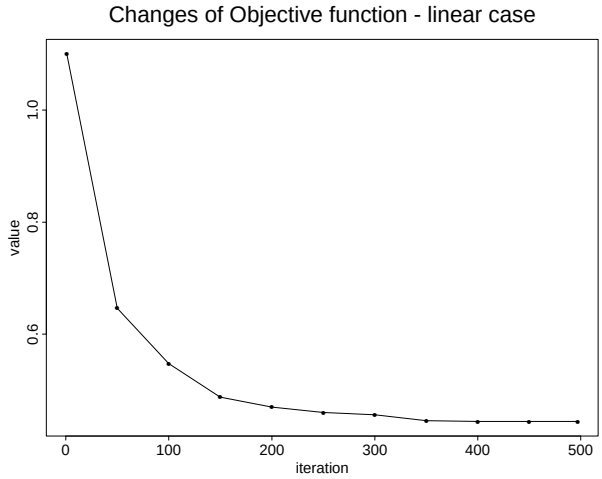

Figure 4: Change of the objective function according to iterations for the linear case of of xample 6.1.

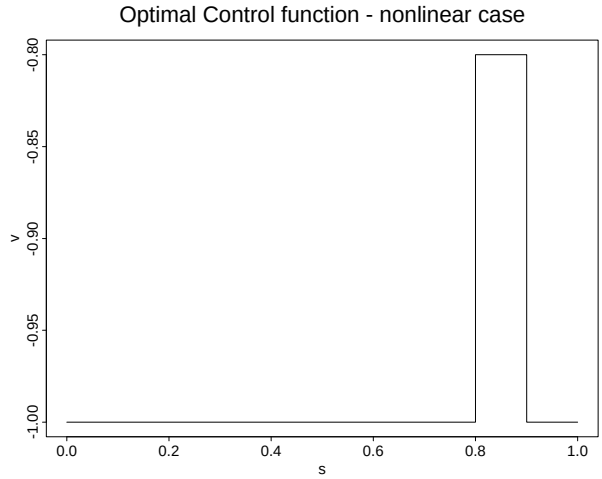

Figure 5: The optimal boundary control function for the nonlinear case of xample 6.1.

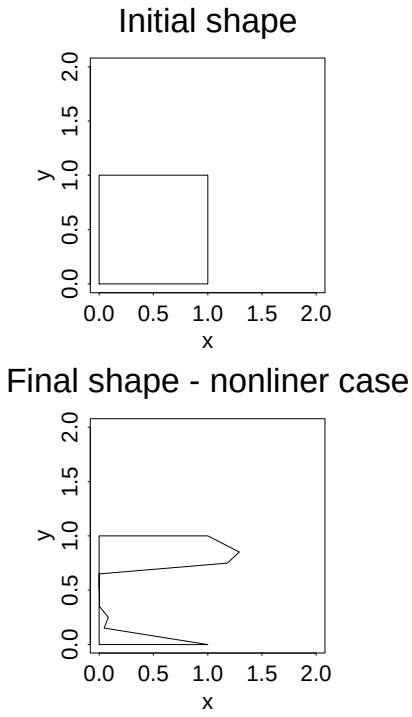

Figure 6: The initial and the optimal domain for the nonlinear case of x-ample 6.1.

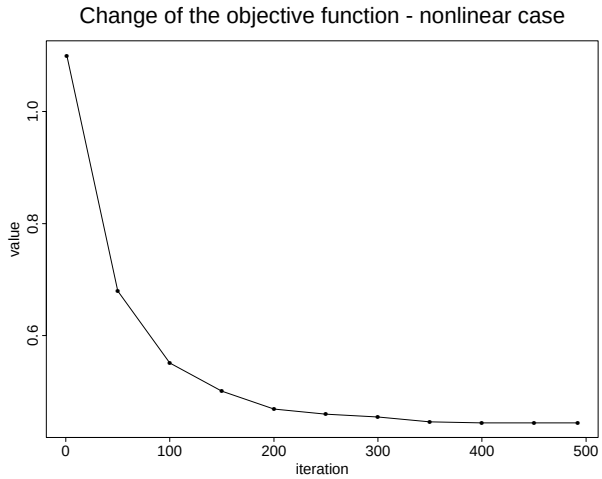

Figure 7: Change of the objective function according to iterations for the nonlinear case of xample 6.1.

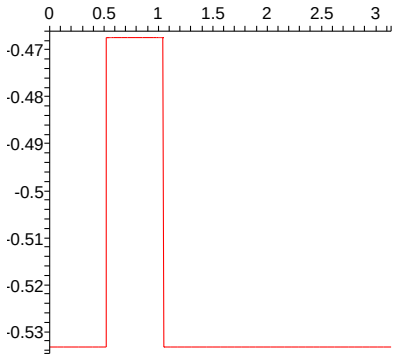

Figure 8: The optimal boundary control function for the linear case of x-ample 6.2.

we have $G_i = v\sqrt{1-y^2}\psi_{ix} - vy\psi_{iy}$. To show that the method is suitable enough even for the hard situations, we considered much more difficulties in conditions. Therefore, it is supposed that here the variables x_i's have an upper bounds $\sqrt{1-Y_i^2}$ and a lower bound which guaranteed that the variable points can not pass the left half of the unite circle. These conditions are applied by means of the penalty method (see [22]). By selecting

$$f_2(s,v) = \begin{cases} \sqrt{(X_i + 5(X_i - X_{i-1})(s - Y_{i-1})^2 + s^2}, & Y_{i-1} \le s \le Y_i \\ s^2 - v^2 - 1, & 1 \le s \le 1 + \pi, \end{cases}$$

$K = 3200$, $N = 11875$, $M_2 = 9$ and $M_3 = 15$ (9 equation for fixed boundary and the rest for Γ), an extra condition for the summation of α_i's is also considered to be sure that the domain is covered by characteristic functions perfectly. Thus Ω and ω are discretized by 15075 nodes in which 100 of them was chosen from the fixed part of boundary and also on each segment $A_{m-1}A_m$, 20 nodes was selected. Moreover the subroutines $AMOEBA$ and $DLLRRS$ from the Fortran library were used for solving the following examples.

inear Case: Let $f_1 = 1 - u^2$ and $f = 0$ (hence the elliptic equation (1) is linear). The initial domain is selected as complete unite circle. After 785 iterations, the optimal value was converge to 19.9850134 and the optimal values of x_i's were: 0.941, 0.1868, 0.2767, 0.3863, 0.5033, 0.3845, 0.2770, 0.1870, 0.0945. The nearly optimal control and the optimal domain, before and after fitting a smooth curve by means of the natural cubic Spline, were plotted in Figures 8, 12 and 10 (by use of Maple9.5 software).

Nonlinear Case: By the above assumptions and choosing $f_1 = x+y+u-0.1$ and $f = 5u^2$, a nonlinear case of the problem is solved. The initial domain is

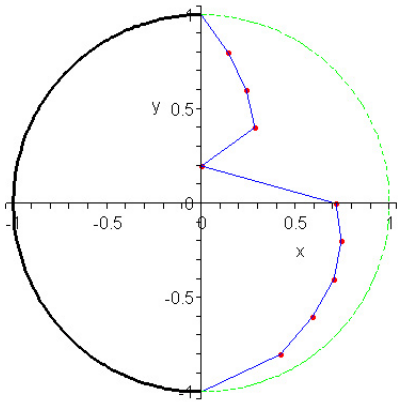

Figure 9: The optimal domain for the linear case of xample 6.2 before fitness.

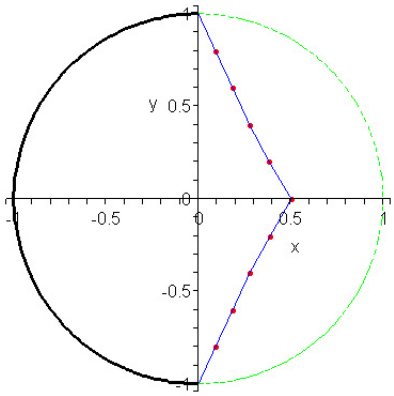

Figure 10: The optimal domain for the linear case of xample 6.2 after fitness.

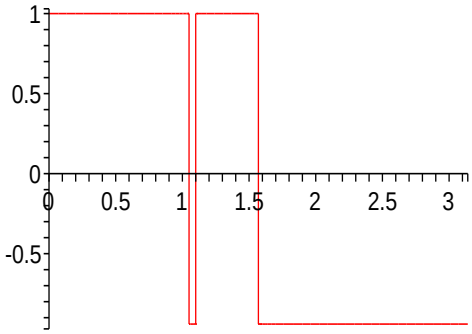

Figure 11: The optimal boundary control function for the nonlinear case of xample 6.2.

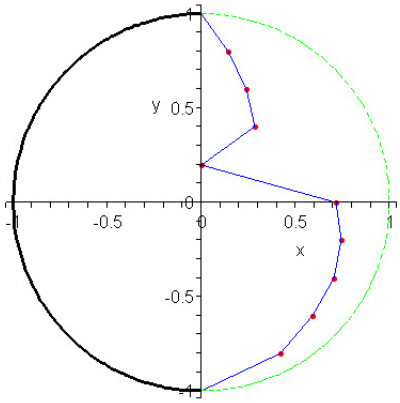

Figure 12: The optimal domain for the nonlinear case of xample 6.2 after fitness.

also selected as a unit circle and after 1303 iterations the optimal control and the optimal domain are obtained. The optimal control is plotted in Figure 11 and after fitting a smooth curve as above, the optimal domain for this case is shown in Figure 12. In this case, the optimal value was 10.699029.

7 Conclusions

Having continued our previous work; herein, we have shown that the mentioned Shape-measure method can be successfully applied for solving free boundary problems which involved with boundary control function. The method was able to characterize the optimal pair of domain and its related

control function simultaneously; moreover, the optimal value for the general form of the objective function were determined in an easy way just by applying a standard search technique and also the simplex algorithm perfectly well. Presenting a linear treatment even for the extremely nonlinear problems was one of the main advantages of this method.

Acknowledgements

The author is very grateful to Prof. Rubio for his valuable comments and all his help.

ist of symbols
D: a domain
∂D: boundary of D
u: solution of the elliptic system
v: boundary control
$\mathcal{D}_{\mathcal{M}}$: the set of admissible domains for fixed M
$\mathcal{D}$: the set of general admissible domains
$\mathbf{F}$: the set of all pairs of (D, v) where $D \in \mathcal{D}_M$
$\mathbf{n}$: is the outward unit vector on ∂D
$H^1(D)$: the Sobolev space of order 1
$H_0^1(D)$: set of functions in $H^1(D)$ in which they are zero on ∂D
$C(\Omega)$: the set of continuous and bounded functions on Ω
$C_1(\Omega)$: the set of functions in $C(\Omega)$ which depend only on the first variable
$\mathcal{M}^+(\Omega)$: the space of positive Radon measures on $C(\Omega)$
$P(x, y)$: the space of polynomials of x and y.

References

1. Alt, W. and Dembo, M. *Cytoplasm dynamics and cell motion: two-phase flow models*, Int. J. Mathematical Biosciences, 156 (1999), 207–228.

2. Berger, M. P. F. and Wong, W. . *Apllied Optimal Designs*, John Wiley & Sons Ltd, 2005.

3. Fakharzadeh Jahromi, A. and Rubio, J. . *Shapes and Measures*, Journal of Mathematical Control and Information, 16 (1999), 207-220.

4. Fakharzadeh Jahromi, A. and Rubio, J. . *Shape-Measure Method for Solving Elliptic Optimal Shape Problems (Fixed Control Case)*, Bulletin of the Iranian Mathematical Society, 27 (2001), 41–63.

5. Fakharzadeh Jahromi, A. and Rubio, J. . *Best Domain for an Elliptic Problem in Cartesian Coordinates by Means of Shape-Measure*, AJOP Asian J. of Control, 11, 5 (2009), 536–547.

6. Farahi, M. H. *The Boundary Control of the Wave Equation*, PhD thesis, Leeds University (1996).

7. Goberna, M. A. and Lopez, M. A. *Linear Semi-infinite Optimization*, Alicant Uiniversity, 1998.

8. Hadamard, J. *Lessons on the Calculus of Variation*. Gauthier-Villards, Paris, 1910. (in French).

9. Haslinger, J. and Neittaanamaki, P. *Finite Element Approximation for Optimal Shape Design: Theory and Applications*, Johan Wiley & Sons Ltd, 1988.

10. Haug, . J. and Cea, J. *Optimization of Disstributed Parameter Structures*, Vols I and II, Sijthoff and Noordhoff, Alpen and Rijn, The Netherland, 1981.

11. amyad, A. V., Rubio, J. . and Wilson, D. A. *The optimal control of multidimensional diffusion equation*, JOTA, 1, 70 (1991), 191–209.

12. Lancaster, . . *Qualitative behavior of solution of elliptic free boundary problems*, Pacific J. Maths., 154, 2 (1992), 297–317.

13. Mikhailov, V. P. *Partial Differential Equation*, MIR Publisher, Moscow, 1978.

14. Munch, A. *Optimal design of the support of the control for the 2-d wave equation: Numerical investigation*, Mathematical Modeling and Numerical Analysis, 5, 2 (2008), 331–351.

15. Munch, A. *Optimal internal dissipation of a damped wave equation using a topological approach*, Int. J. Appl. Math. Comput. Sci., 19, 1 (2009), 15–37.

16. Nelder, J. A. and Mead, R. *A simplex method for function minimization*, The Computer Journal, 7 (1964-65), 303-313.

17. Press, W. H.,Teukolsky, S. A., Vetterling, W. T. and Flannery, B. R. *Neumerical Recipes in Fortran: The art of scientific computing*, 2ed edition, Cambridge unversity press, 1992.

18. Pironneau, O. *Optimal Shape Design for Elliptic System*, Springer-Verlag, New York - Berlin - Heidelberg - Tokyo, 1983.

19. Rubio, J. . *Control and Optimization: The Linear Treatment of Nonlinear Problems*, Manchester University Press, Manchester, 1986.

20. Rubio, J. . *The global control of nonlinear elliptic equation. Journal of Franklin Institute*, 330, 1 (1993), 29–35.

21. Rudin, W. *Real and Complex Analysis*, Tata McGraw-Hill Publishing Co.Ltd, New Delhi, second edition, 1983.

22. Sun, W. and Ya-Xiang, X. *Optimization Theory and Methods: Nonlinear programming*, Springer, 2006.

23. Vogel, T. *A free boundary problem arising from galvanizing process*, SIAM J. Math. Mech. Anal., 16 (1985) 970–979.

24. Young, L. C. *Lectures on the Calculues of Variations and Optimal Control Theory*, W.B. Sunders Company, 1969.

Iranian J. of Numerical Anal sis and Optimization
Vol 3, No. 2, 2013 , pp 67-77

Relation between intersection of nullclines and periodic solutions in a differential equations of p53 oscillator

F. Rangi and M. Tavakoli

Abstract

We consider a simple mathematical model that suggests emergence of oscillations in p53 and Mdm2 protein levels in response to stress signal. Intracellular activit of the p53 protein is regulated b a transcriptional target, Mdm2, through a feedback loop. The model is classified in five cases ith respect to intersection of nullclines. In each case occurrence or not of the limit c cle is investigated.

ey ords: DNA damage; p53-Mdm2; Limit cycle; Mathematical biology.

1 Introduction

The p53 protein is suppressor tumor that plays an important role in growth, arrest, senescence, and apoptosis in response to broad array of cellular damage.In more than 50% of human cancer, the p53 is muteted[3]. Under normal, unstressed conditions (for example calls dont suffer DNA damage or no DNA damage) the concentration of p53 is kept at low levels by Mdm2 gene. Mdm2 plays a key role in preserving p53 levels low in normal cell while the Mdm2 transcription is induced by p53 itself[3]. Thus with negative feedback loop ($p53 \rightarrow Mdm2 \dashv p53$) any increase of p53 normally leads to an increase in Mdm2 levels, which then pushes p53 back down to a low steady state level[7]. But In environmental stresses such as DNA damage, the concentration of p53 increase and inducing a transition to oscillations of p53 level [4]. Namely p53 arrests the cell cycle, thereby giving the cell time to correct any DNA damage, activates transcription of genes which is indirectly responsible to DNA repair, and can be the cause of apoptosis [2]

Lahava et al. in [8] measured intercellular concentration of total p53 and Mdm2 protein and observed p53 and Mdm2 protein concentration in a

Recieved 19 Februar 2013; accepted 12 June 2013
Fahimeh Rangi
Department of Applied Mathematics, Ferdo si niversit of Mashhad, Mashhad, Iran,
e-mail f_rangi ahoo.com

Mahboobeh Tavakoli
ardis of Hashemine ad, Farhangian niversit , Mashhad, Iran.
e-mail math.tavakoli gmail.com

single cell oscillation in response to DNA damage, and proposed that system behaved as a digital oscillator [2].

The generation of oscillations in the p53/Mdm2 network seems a challenge to modellers, becuase negative feedback is not sufficient for oscillatory behaviors. For example, a negative feedback composed of only two elements, such as $p53 \rightarrow Mdm2 \dashv p53$, cannot oscillate. The observation of *Lahava et al.* in [8] leads to several interesting model and hypotheses [3, 9]. In fact several mathematical models have been proposed to explain the damped oscillations of p53, either in cell population or in a single cell, most of which are deterministic models of ordinary differential equations [15]. *Lev Bar Or et al.* considered the possibility of a negative feedback loop composed of three components (Mdm2, p53 and putative intermediate factor), which can oscillate (part A of Figure1) or require the simultaneous presence of negative and positive feedbacks (part B of Figure1)[3] .

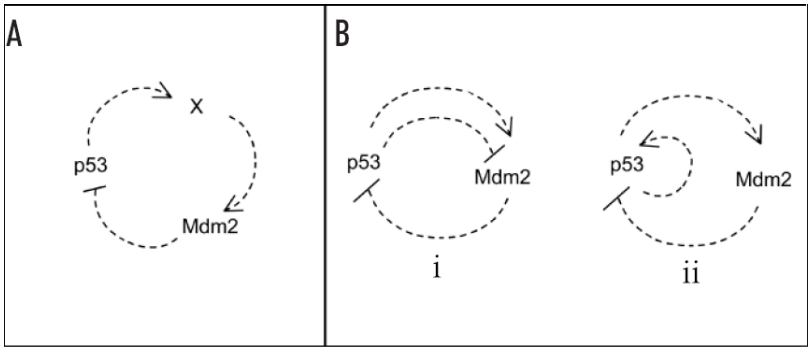

Figure 1: Pathways to oscillations. Oscillation can be found in two different types (A) negative feedback loops with three or more components and (B) combinations of negative and positive feedbacks

Tyson in response the observation of *Lahava* which showed the digital oscillator behavior, assumed the steady state p53 concentration passes through a hopf bifurcation in following DNA damage and the p53 and Mdm2 levels begin to oscillate [2, 15]. In [2]another protein (The Atm protein) has been mentioned that is similar to a switch that caused the p53- Mdm2 oscillator be into or out to oscillatory zone. By following to in[12] regions of parameters into which the Atm protein can switch off damage signals, are determined.

Another approach to modeling the p53 dynamics make explicit use of delays in the system corresponding to the time that it takes for transcription and translation of proteins [10, 14, 16].

Consider two types of motifs, as illustrated in Figure1, which are discussed in [3]. Case ii in part B of Figure1 has autocatalysis in p53, whereas in case i of that figure, in addition to the normal activation of Mdm2 by p53, there is a path by which Mdm2 is down-regulated by p53 [2].

A recent elementary model which is motivated biologically according to case ii in part B of Figure1 (autocatalysis) formulates as below

$$\begin{cases} \dot{x} = & \alpha_0 + \dfrac{\alpha_1 x^n}{k_1 + x^n} - \gamma_1 xy - \gamma_2 x = F \\ \dot{y} = & \alpha_2 + \dfrac{\alpha_3 x^4}{k_2 + x^4} - \gamma_3 y = G \end{cases} \tag{1}$$

where $x(t) = [p53(t)]$ and $y(t) = [Mdm2](t)$ are denoting concentration of p53 and Mdm2 respictively[2]. In the first equation above,α_0 shows the production rate of p53, the second therm with coefficient α_1 represents an autocatalytic process and it is described with a Hill coefficient $n \in N$ which determines the degree of cooperativity of the ligand of p53 binding to the enzyme or receptor [5]. The third therm represents the active process of ubiquitination of p53 independently of Mdm2 and the fourth term represents the degradation of p53 independently of Mdm2. Similarly in the second equation above, α_2 shows the production rate of Mdm2, and second term with coefficient α_3 represents the activation of Mdm2 by p53 whit Hill coefficient 4, and the third represents the degradation of Mdm2 [2] .

Analysis the trace and determinate of system (1) can be shown in addition to negative feedback loop in p53 - Mdm2 network, autocatalysis by either p53 or Mdm2 leads to the possibility of oscillatory behavior. In the absence of autocatalysis, one can still get oscillations if p53 also down-regulates Mdm2 or Mdm2 also up-regulates p53, in addition to the normal activation.

Here, Oscillatory behavior was described in the form of a limit cycle i.e. to obtain oscillatory behavior from each initial condition the fixed point of the system that resides within the limit cycle needs to be an unstable spiral. In this case all trajectories in the phase plane originating at near that fixed point spiral out and asymptote onto the limit cycle [2].

The goal of system biology is to analyze the behavior and interrelationships of functional biological system [13]. we analyze system (1)) to find out the possible cases for existence of limit cycles that oscillatory behavior in p53-Mdm2 network is described. In fact the DNA damage can be controlled when slightly oscillatory region would be given in system (1). In other word, by changing the parameter values (parameter values to get the oscillation) and conditions are imposed on the system (1), then system has the stable limit cycle (oscillatory mode). Therefore, giving cell time to the repair the damage and will not develop cancer. For this purpose we use the Poincare Bendixson Theorem that possible case are shown for existence or nonexistence of limit cycle in system (1). The Poincare Bendixson theorem says that as $t \to \infty$ the trajectories will tend to a limit cycle solution[11].

Theorem 2. *(***Poincare endixson Theorem***) Suppose that* Ω *is a nonempty, closed and bounded limit set of a planar of differential equation that contains no equilibrium point. Then* Ω *is a closed orbit [6].*

On of the most useful tools for analyzing nonlinear systems of differential equations (especially planer systems) are the nullclines. For a system in the form

$$\begin{cases} \dot{x}_1 = & f_1(x_1, x_2, \cdots, x_n) \\ \vdots & \\ \dot{x}_n = & f_n(x_1, x_2, \cdots, x_n) \end{cases} \tag{2}$$

The x_j -nullcline is the set of points where $\dot{x}_j$ vanishes, so the x_j -nullcline is the set of points determined by setting $f_j(x_1, x_2, \cdots, x_n) = 0$ [6].
First, with regard to the intersections of x- and y- nullcline (equilibrium point) of system (1), We classify them in several cases. In any of regions between the nullclines, the vector field is neither vertical nor horizontal, so it must point in one of four direction: northeast, northwest, southeast or southwest. We call such regions **basic region** [6]. The basic regions where $\dot{x} \neq 0$ and $\dot{y} \neq 0$ are of four types:

$$\text{A:}\dot{x} > 0, \dot{y} > 0 \ \text{B:}\dot{x} < 0, \dot{y} > 0$$
$$\text{C: } \dot{x} < 0, \dot{y} < 0 \ \text{D:}\dot{x} > 0, \dot{y} < 0$$

quivalently, these are the regions where the vector field points northeast, northwest, southwest, or southeast, respectively. [6].

Next we investigate the possibility of existence or nonexistence of limit cycles in system (1) by using Poincare Bendixson theorem. The Poincare Bendixson theorem says when the trajectory will tend to a limit cycle solution as $t \to \infty$.

2 Classifying of nullclines

x- nullcline in system (1) is the set of points where $F(x, y) = 0$.

$$F(x, y) = 0 \Longrightarrow y = f(x) = \frac{1}{\gamma_1}(\frac{\alpha_0}{x} + \frac{\alpha_1 x^{n-1}}{k_1 + x^n} - \gamma_2) \tag{3}$$

The map $y = f(x)$ has two critical point

$$x_{1,2} = \sqrt[n]{\frac{k_1(-2\alpha_0 + \alpha_1(n-1) \pm \sqrt{q})}{2(\alpha_0 + \alpha_1)}} \tag{4}$$

where

$$q = -4n\alpha_0 + \alpha_1^2 n^2 - 2\alpha_1^2 n + \alpha_1^2 \tag{5}$$

If we assume that x_1 and x_2 are positive, real and different; Therefore q must be positive. It is easy to see that $x_1 > x_2$.

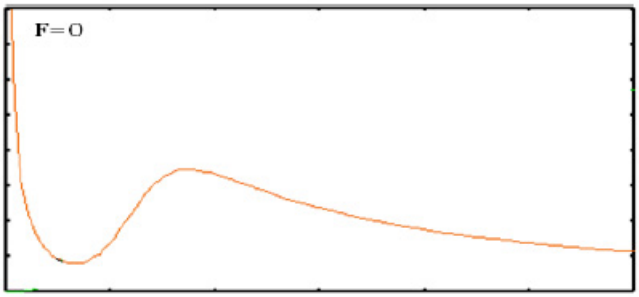

Figure 2: x-nullcline

So if $x \to 0$, then $f(x) = y \to \infty$. Since the x_1 and x_2 are positive and $x_1 > x_2$ then sign f' is negative in interval $(0, x_2)$ and the map y=f(x) is decreases in this area. The sign of f' is changed in x_2 because x_1 and x_2 are simple roots of equation $y = f'(x)$. Therefore sign f' is positive between x_1 and x_2 and the map y=f(x) is increases in (x_2, x_1). The map has a change of sign in x_1, so sing f' is negative in (x_1, ∞) and $y = f(x)$ is decreasing in this interval. Therefore x_1 and x_2 are maximum and minimum for $y = f(x)$, respectively.

Also, for the graph of G(x,y)=0 i.e. y - nullcline We have

$$G(x, y) = 0 \Longrightarrow y = g(x) = \frac{1}{\gamma_3}\left(\frac{\alpha_3 x^4}{k_2 + x^4} + \alpha_2\right) \tag{6}$$

and

$$\lim_{x \to 0} g(x) = \frac{\alpha_2}{\gamma_3}, \lim_{x \to +\infty} g(x) = \frac{\alpha_3}{\gamma_3} \tag{7}$$

and

$$g'(x) = \frac{1}{\gamma_3}\Big(\frac{4\alpha_2 k_2 x^3}{(k_4 + x^4)^2}\Big) \tag{8}$$

So $g'(x) > 0$ in the first region coordinate system $(x > 0, y > 0)$. Therefore g(x) increases in this region

Now with regard to the intersections of x- and y- nullclines of system (1), it is classified in several cases and we obtained the vector field for each of these cases by XPP software. We discussed possibility of existence or nonexistence of limit cycle near the equilibrium point (intersection of nullclines).

Case 1: The intersection before minimization
In this case,Trajectory of solution tends to intersection point of nullclines and system do not have limit cycle near the intersection point(Figure 4). The vector field is plotted for these parameters in this figure. By the basic region, as mentioned in introduction, the sign of $\dot{x}$ and $\dot{y}(F$ and $G)$ can be determined respectively. We use the direction of vector field and basic regions

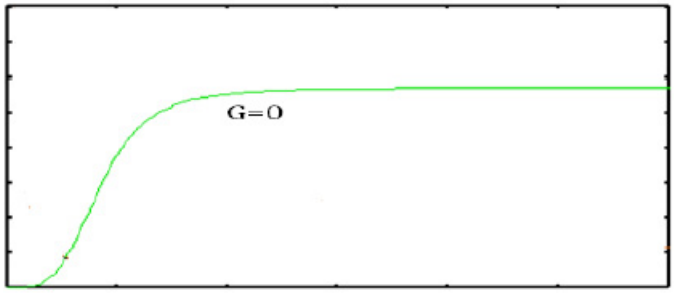

Figure 3: y-nullcline

to get the sing of F_y and F_x and G_x and G_y for Jacobin matrix system(1) in intersection point .

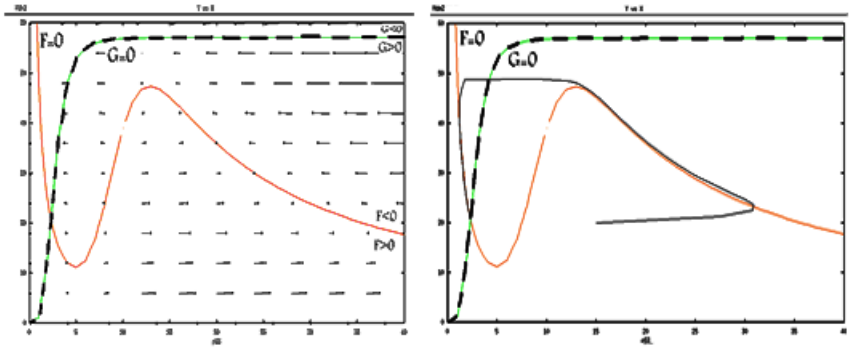

Figure 4: The vector field and nullclines and trajectory solution for the first case

$$\mathbf{A} = \begin{pmatrix} F_x(x_s, y_s) & F_y(x_s, y_s) \\ G_x(x_s, y_s) & G_y(x_s, y_s) \end{pmatrix} \tag{9}$$

We move a long a line parallel to the x-axis through the equilibrium point , F decreases since $F > 0$ the lower x-side and $F < 0$ on the higher x-side. Therefore, Sign of F_x is negative. Similarly, we move a long a line parallel to the y-axis through the equilibrium point , G decreases since $G > 0$ the lower y-side and $G < 0$ on the higher y-side (for detail see [11]). Therefore, Sign of G_y is negative. So x- and y -nullcline is decrease and increase in intersection point respectively. As we have in near the equilibrium point

$$\frac{dx}{dy}]_{F=0} = -\frac{F_y}{F_x} < 0, F_x < 0 \Rightarrow F_y < 0 \tag{10}$$

$$\frac{dx}{dy}]_{G=0} = -\frac{G_y}{G_x} > 0, G_y < 0 \Rightarrow G_x > 0 \tag{11}$$

In this case, sign of Jacobin matrix is equal

$$\mathbf{A} = \begin{pmatrix} - & - \\ + & - \end{pmatrix} \tag{12}$$

Therefore trace of A matrix is negative and eigenvalues of A matrix is equal

$$\lambda_{1,2} = \frac{trA}{2} \pm \frac{1}{2}\sqrt{(trA)^2 - 4detA} \tag{13}$$

The equilibrium point is stable since eigenvalue of system (1) is negative real part. Therefore system (1) by the Poincare Bendixson Theorem do not have limit cycle near the intersection point in this case.

Case 2: the intersection after maximization of graph F=0

The vector field is plotted in Figure 5. By a similar process in the first case,

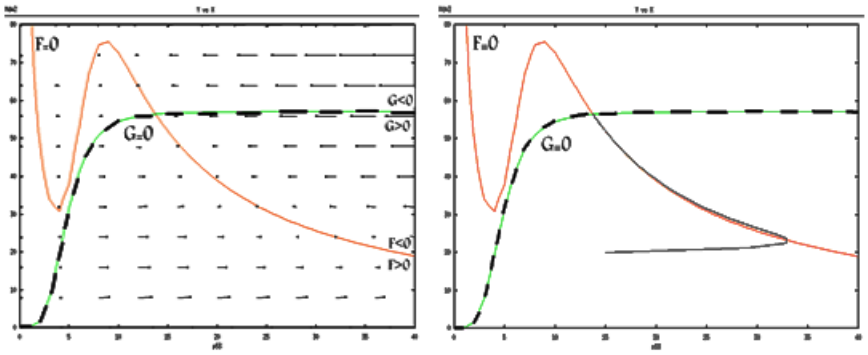

Figure 5: The vector field and nullclines and trajectory solution for the second case

the sign at A matrix is equal

$$\mathbf{A} = \begin{pmatrix} - & - \\ + & - \end{pmatrix} \tag{14}$$

which is $tr\mathbf{A} < 0$ and eigenvalue of system is negative real part. Therefore the equilibrium point is stable. So system (1) do not have limit cycle near the intersection point in this case.

Case 3: the intersection bet een maximum and minimum of graph F=0
Figure 6 showes the vector field in this case. Similarly we have

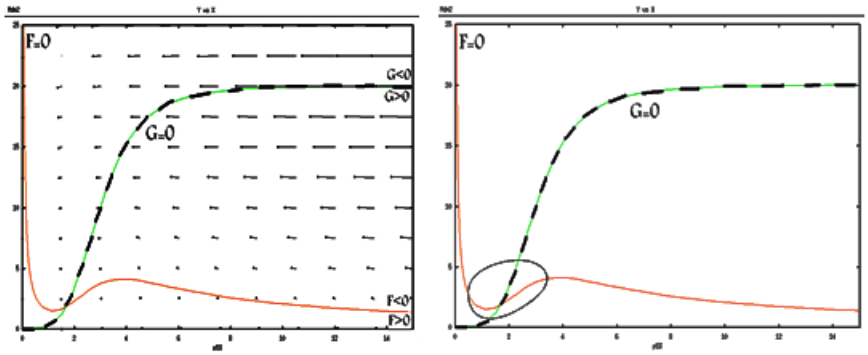

Figure 6: The vector field and nullclines and trajectory solution for the third case

$$\mathbf{A} = \begin{pmatrix} + & - \\ + & - \end{pmatrix} \tag{15}$$

In this case, it is possible that system (1) admits periodic solution [11]. We plotted the limit cycle near the intersection point in Figure 6 .

Case 4: t o intersection points
We observe that system has two stable intersection points, which S_1 point is similar to first case. So system (1) has not limit cycle near the intersection point in this case.

Case : three intersection points (after maximum, bet een maximum and minimum, before minimum)
In Figure 8, S_1 and S_3 points are located before of x_2 and after of x_1 respectively. Thus system (1) don't have limit cycle near these points, because S_1 and S_2 are stable points.
For S_2 we have

$$F_x > 0, F_y < 0, G_x > 0, G_y < 0 \tag{16}$$

$$0 < \frac{dy}{dx}\Big]_{G=0} < \frac{dy}{dx}\Big]_{F=0} \Rightarrow 0 < -\frac{G_x}{G_y} < -\frac{F_x}{F_y}. \tag{17}$$

So

$$det(A) = F_x G_y - F_y G_x < 0. \tag{18}$$

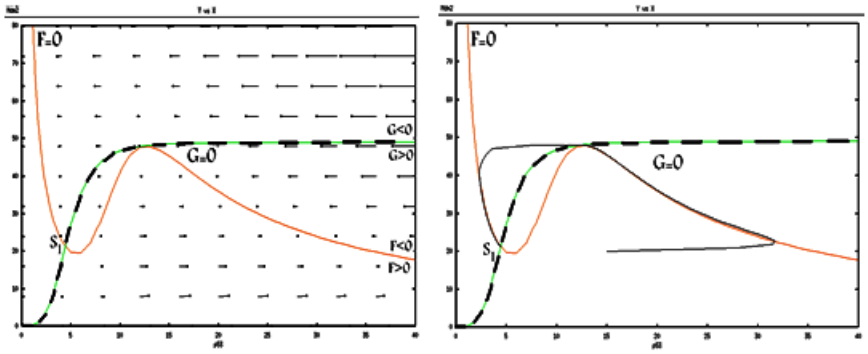

Figure 7: The vector field and nullclines and trajectory solution for the fourth case

This shows that S_2 is saddle point. According to the Poincare Bendixson theorem, this type of singularity does not admit periodic solutions. For more details see([11]Section 7.3)

In following theorem we prove analytically that the only possible case for the existence of limit cycle is second case and other cases don't have limit cycle at all.

Theorem 3. ***Theorem:****System (1) can not admit limit cycle in cases 1, 2, 4 and 5 for the positive value of* γ_1, γ_3 *and* x_s*(intersection point of nullclines).*

Proof. If (x_s, y_s) is equilibrium point of system (1) then Jocobian matrix of system (1) is equal

$$\mathbf{A} = \begin{pmatrix} F_x(x_s, y_s) & F_y(x_s, y_s) \\ G_x(x_s, y_s) & G_y(x_s, y_s) \end{pmatrix} \tag{19}$$

and eigenvalues of matrix A are

$$\lambda_{1,2} = \frac{trA}{2} \pm \frac{1}{2}\sqrt{(trA)^2 - 4detA} \tag{20}$$

By $G_x = -G_y \dfrac{dg}{dx}$ and $F_x = -F_y \dfrac{df}{dx}$ we have

$$det(A) = F_x G_y - F_y G_x = -F_x G_y \frac{df}{dx} + F_y G_y \frac{dg}{dx} \Rightarrow det(A) = F_y G_y (g' - f') \tag{21}$$

Also

$$F_y = -\gamma_1 x, G_y = -\gamma_3 \tag{22}$$

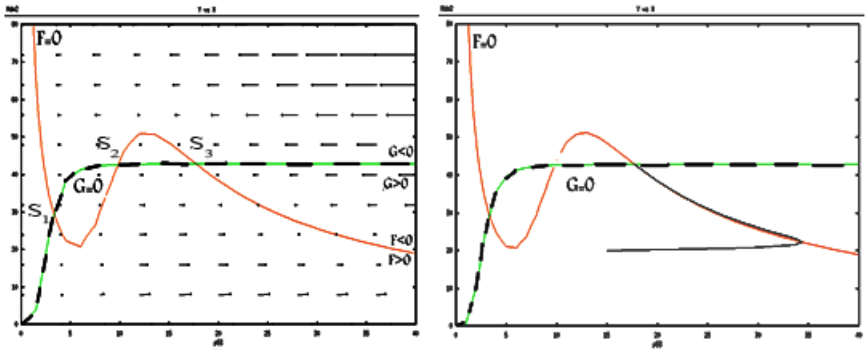

Figure 8: The vector field and nullclines and trajectory solution for the fifth case

Then

$$\lambda_{1,2} = \frac{\gamma_1 x_s f'(x_s) - \gamma_3 \pm \sqrt{(\gamma_1 x_s f'(x_s) - \gamma_3)^2 - 4\gamma_1\gamma_3 x_s (g'(x_s) - f'(x_s))}}{2} \tag{23}$$

Now since the (x_1, y_1) point is maximum of map f, if the intersection occurs after maximum point then $f'(x_i) \leq 0$ for each of x_i that $x_i \geq x_1$. Hence we have $f'(x_s) \leq 0$, so by the positive value of γ_1, γ_3 and x_s, $trA < 0$ and the (x_s, y_s) point is stable point. Therefore trajectory of solution limits to that point and we don't have limit cycle near this point.
Similarly if the intersection of maps f and g occurs before minimum of map f then the trace of matrix A is negative because of we have $f' \leq 0$ in interval $(0, x_2]$ and so this point is a stable point that trajectory of system (1) limits to that point. □

References

1. Bar-Or, R. L., Maya, R., Segel, L. A., Alon, U., Levine, A. J. and Oren, M. *Geneneration of oscillations by the p*53*-Mdm*2 *feedback loop:Atheorical and experimental study*, Departements of Molecurlar Cell Biology and Applied Mathematics and Computer Scince, 97 (2000), 11250–11255.

2. Chicarmane,V., Ray,A., Sauro, H. M. and Nadim, A. *A model for p*53 *dynamics trigged by DNA damage*, SAIM J.Applied Dynamicals systems, 6 (2007), 1, 61–78.

3. Ciliberto, A., Novake, B. and Tyson, J.J. *Steady States and Oscillations in the p53/Mdm2 Network* Cell Cycle 4:3. , 130 (2005), 488–493.

4. Ge H. and Qian, M. *Boolean Network Approach to negative Feedback Loops of the p53 Pathways: Synchronized Dynamics and stochatics Limit cycle*, Jornal of computation biology, 6, 1 (2009), 119–132.

5. Hill, A. V. *The possible effects of the aggregation of the molecules of hamoglobin on its dissosiation curves*, J. Physiol., 40 (1910), 4–7.

6. Hirsch, M. W., Smale, S. and Devaney, R. L. *Differntial equation , dynamical systems and introduction to chaos*, second edition, lsevier, USA, 2004.

7. Lahva, G. *Oscillations by the p53-Mdm2 feedback loop*, Journal of Construction ngineering and Manage-ment, 131 (2005), 1115–1123.

8. Lahva, G., Rosenfeld, N., Sigal, A., Geva-Zatorsky, N., Levine, A.J., lowitz, M. B. and Alon, U. *Dynamics of the p53-Mdm2 feedback loop in the individual cells*, Nature Genetics, 36 (2004), 147–150.

9. Ma, L., Wangner, J., Rice, J. J., Hu, W., Levvien, A. J. and Storlovitzky, A. *A plausible model for the digital response of p53 to DNA damage*, Proc. Nat. Acad. Scien., 102 (2005), 14266–14271.

10. Monk, N. A. M. and Rice, J. J.*Oscillatory expression of Her1, p53, and NF-kappaBdriven by transcriptional time delays*, Current Biology, 97 (2000), 11250–11255.

11. Murray, J. D. *Matematical Biology* ,3rd edition, Springer-Verlag Berlin Heidelberg, 1991.

12. Rabiei motlagh, O. and Afsharnezhad, Z. *On the conditions for which the Atm protein switch off the DNA damage signal in a p53 model*, Studia Universitatis BAbes- Bolyal, Biologia, 1 (2010), 67–79.

13. Sauro, H., Adelinde, M., Uhrmacher, M., Harel, D., Hucka, M., wiatkowska, M., Mendes, P., Shaffer, C. A., Stromback, L. and Tyson, J. J. *Challenges for modeling and simulation methods in systems biology*,Proceedings of the 2006 Winter Simulation Conference, 67–79.

14. Tiana, G., Jensen, M. H. and Sneppen, . *Time delay as a key to opoptosis induction in the p53 network*, uro. Phys. j., 39 (2002), 135–140.

15. Tyson, J. J. *Monitoring p53's pulse*, Nature Genetics, 36 (2004), 113–114.

16. Wangner, J., Ma, L., Rice, J. J., Hu, W., levvien, A. J. and Storlovitzky, A. *p53-Mdm2 loop controlled by abalance of its feedback strenght and effective dampening using Atm and delayed feedback*,I Proc. System Biology., 152 (2005), 109–118.

Aims and scope

Iranian Journal of Numerical Analysis and Optimization (IJNAO) is published twice a year by the Department of Applied Mathematics, Faculty of Mathematical Sciences, Ferdowsi University of Mashhad. Papers dealing with different aspects of numerical analysis and optimization, theories and their applications in engineering and industry are considered for publication.

Journal Policy

After receiving an article, the editorial committee will assign referees. Refereeing process can be followed via the web site of the Journal.
The manuscripts are accepted for review with the understanding that the work has not been published and also it is not under consideration for publication by any other journal. All submissions should be accompanied by a written declaration signed by the author(s) that the paper has not been published before and has not been submitted for consideration elsewhere.

Instruction for Authors

The Journal publishes all papers in the fields of numerical analysis and optimization. Articles must be written in English.
All submitted papers will be refereed and the authors may be asked to revise their manuscripts according to the referee's reports. The Editorial Board of the Journal keeps the right to accept or reject the papers for publication.
The papers with more than one authors, should determine the corresponding author. The e-mail address of the corresponding author must appear at the end of the manuscript or as a footnote of the first page.
It is strongly recommended to set up the manuscript by Latex or Tex, using the template provided in the web site of the Journal. Manuscripts should be typed double-spaced with wide margins to provide enough room for editorial remarks.
References should be arranged in alphabetical order by the surname of the first author as examples below:
[1] Stoer, J. and Bulirsch, R. *Introduction to Numerical Analysis*, Springer-verlag, New York, 2002.
[2] Brunner, H. *A survey of recent advances in the numerical treatment of Volterra integral and integro-differential equations*, J. Comput. Appl. Math. 8 (1982), 213-229.

Submission of Manuscripts

Authors may submit their manuscripts by either of the following ways:

a) Online submission (pdf or dvi files) via the website of the Journal at:

http://jm.um.ac.ir/index.php/math

b) Via journal's email mjms@um.ac.ir

Copyright Agreement

Upon the acceptance of an article by the Journal, the corresponding author will be asked to sign a "Copyright Transfer Agreement" (see the web site) and send it to the Journal address. This will permit the publisher to publish and distribute the work.

Iranian Journal of Numerical Analysis and Optimization

Former : MRJMS

CONTENTS Vol. 3, No.2, pp 1-77, 2013

web site : http://jm.um.ac.ir

Email : mjms@um.ac.ir

ISSN : 1735-7144